# Mixed ligand ruthenium(II) complexes of bis(pyrid-2-yl)-/bis(benzimidazol-2-yl)-dithioether and diimines: Study of non-covalent DNA binding and cytotoxicity†‡

**Venugopal Rajendiran,[a] Mariappan Murali,§[a] Eringathodi Suresh,[b] Sarika Sinha,[c] Kumaravel Somasundaram[c] and Mallayan Palaniandavar*[a]**

***Received 11th July 2007, Accepted 19th September 2007***
***First published as an Advance Article on the web 11th October 2007***
**DOI: 10.1039/b710578a**



A series of mixed ligand ruthenium(II) complexes [Ru(pdto)(diimine)]$(ClO_4)_2$/$(PF_6)_2$ **1–3** and [Ru(bbdo)(diimine)]$(ClO_4)_2$ **4–6**, where pdto is 1,8-bis(pyrid-2-yl)-3,6-dithiooctane, bbdo is 1,8-bis(benzimidazol-2-yl)-3,6-dithiooctane and diimine is 1,10-phenanthroline (phen), dipyrido-[3,2-*d*:2′,3′-*f*]-quinoxaline (dpq) and dipyrido[3,2-*a*:2′,3′-*c*]phenazine (dppz), have been isolated and characterised by analytical and spectral methods. The complexes [Ru(pdto)(phen)]$(PF_6)_2$ **1a**, [Ru(pdto)(dpq)(Cl)]$(PF_6)$ **2a**, [Ru(bbdo)(phen)]$(PF_6)_2$ **4a** and [Ru(bbdo)(dpq)]$(ClO_4)_2$ **5** have been structurally characterized and their coordination geometries around ruthenium(II) are described as distorted octahedral. In **1a**, **4a** and **5** the two thioether sulfur and two py/bzim nitrogen atoms of the tetradentate pdto/bbdo ligand are folded around Ru(II) to give predominantly a "*cis*-α" configuration. $^1$H NMR spectral data of the complexes support this configuration in solution. In [Ru(pdto)(dpq)Cl]$(PF_6)$ **2a** with a distorted octahedral coordination geometry, one of the two py nitrogens of pdto is not coordinated. The DNA binding constants ($K_b$: **2**, $2.00 \pm 0.02 \times 10^4$ $M^{-1}$, $s = 1.0$; **3**, $3.00 \pm 0.01 \times 10^6$ $M^{-1}$, $s = 1.3$) determined by absorption spectral titrations of the complexes with CT DNA reveal that **3** interacts with DNA more tightly than **2** through partial intercalation of the extended planar ring of coordinated dppz with the DNA base stack. The DNA binding affinities of the complexes increase with increase in the number of planar aromatic rings in the co-ligand, and on replacing both the py moieties in pdto complexes (**1–3**) by bzim moieties to give bbdo complexes (**4–6**). Upon interaction with CT DNA the complexes **1**, **2**, **5** and **6** show a decrease in anodic current in the cyclic voltammograms. On the other hand, interestingly, **3** and **4** show an increase in anodic current suggesting their involvement in electrocatalytic guanine oxidation. Interestingly, of all the complexes, only **6** alters the superhelicity of DNA upon binding with supercoiled pBR322 DNA. The cytotoxicities of the dppz complexes **3** and **6**, which avidly bind to DNA, have been examined by screening them against cell lines of different cancer origins. It is noteworthy that **6** exhibits selectivity with higher cytotoxicity against the melanoma cancer cell line (A375) than other cell lines, potency approximately twice that of cisplatin and toxicity to normal cells 3 and 90 times less than cisplatin and adriamycin respectively.

## Introduction

Designing effective anti-cancer drugs is an active research area in the field of pharmaceutical chemistry. Currently *cis*-diamminedichlorideplatinum(II) (cisplatin) is one of the most widely used antitumor drugs, treating some human cancers with tremendous success but the dose-limiting nephrotoxicity and the development of drug resistance prevents its potential efficacy.[1,2] This provides the impetus to search for metallo-drugs bearing metal ions other than platinum. Ruthenium complexes are regarded as promising alternatives to platinum complexes and several ruthenium complexes have now been proposed as potential anticancer substances,[3] demonstrating remarkable anticancer activity and showing lower general toxicity than platinum compounds.[4,5] Thus the Ru(III) complex ImH[*trans*-$RuCl_4$(DMSO)(Im)], NAMI-A, shows high selectivity for solid tumor metastases[6a,b] (prevents spread of cancer) and low host toxicity[6c–e] and is the first ruthenium complex to enter clinical trials.[6e] However, it fails to affect primary tumor growth[7] and does not exhibit cytotoxicity against tumor cells *in vitro*. A related Ru(III) compound,[8a] KP1019, has also entered clinical trials, as it was found to exhibit antiproliferative activity *in vitro* in human colon carcinoma cell lines.[8b] Very recently, Sadler and his

[a]*School of Chemistry, Bharathidasan University, Tiruchirappalli 620 024, Tamilnadu, India. E-mail: palanim51@yahoo.com*
[b]*Analytical Science Discipline, Central Salt and Marine Chemical Research Institute, Bhavnagar 364 002, India*
[c]*Department of Microbiology and Cell Biology, Indian Institute of Science, Bangalore 560 012, India*

† CCDC reference numbers 653788–653791. For crystallographic data in CIF or other electronic format see DOI: 10.1039/b710578a

‡ Electronic supplementary information (ESI) available: $^1$H NMR spectral data for complexes **1–6** and Fig. S1. See DOI: 10.1039/b710578a

§ Present address: Department of Chemistry, National College, Tiruchirappalli 620 001, Tamil Nadu, India.

 

co-workers reported half-sandwich Ru(II) arene complexes, which exhibit reproducible anticancer activity against A2780 human ovarian cancer cell lines both *in vitro* and *in vivo*.[9] Since DNA has been identified as the possible primary molecular target[10] of metal-based anticancer agents like cisplatin,[1] attention is mainly focused on interacting ruthenium complexes with DNA to identify whether DNA binding is effective and whether they can act as chemotherapeutic agents. All the above complexes have been suggested to exhibit a mode of action different from Pt(II) drugs and the Ru(III) complexes are proposed to be reduced in the hypoxic tumour tissues to more reactive Ru(II) species, which then form DNA adducts contributing to the cytostatic effects.

The mechanism of action of DNA-targeting metal-based drugs has been thought to involve covalent binding to nucleobase moieties and a low degree of selectivity.[11] So, there is considerable attention focused on the design of new metal-based drugs that exhibit enhanced selectivity and novel DNA interaction modes like non-covalent interactions.[12] Very recently non-covalent DNA binding metal complexes,[13a,13b] particularly, metallointercalators have received attention in the development of efficient anticancer drugs.[13c] Intercalation is well-known to strongly influence the properties of DNA and has been reported as a preliminary step in mutagenesis.[14] Also, the mechanism of action of coplanar annealated polycyclic compounds has been suggested to involve intercalation with human B DNA as an endogenous receptor.[14] Dunbar and co-workers have reported that some of the metallointercalators they developed exhibit photocytoxicity.[15] Several Ru(II) complexes[16] containing aromatic diimine ligands like 1,10-phenanthroline (phen) and extended phenanthrolines with large aromatic surface area which can slot themselves in between the DNA base stack, have been studied with an aim to enhance the DNA binding affinity and hence use them as probes for DNA structure.[17] Having been involved in probing the DNA interaction of Ru(II)[16,18a,18b] and Cu(II) complexes,[18c] we focus our attention now on the design and synthesis of ruthenium(II) complexes with ligands displaying strong DNA binding affinity so as to modify the properties of DNA. As we aim to establish the structural foundation for the design of new ruthenium complexes, which possess more potent and intercalative DNA binding, as target specific anticancer agents, we also determine the DNA binding properties of the complexes. Mixed ligand Ru(II) complexes are very good candidates as their structural and electronic properties can be tuned easily by varying both the primary and co-ligands.

In this report we explore the DNA binding properties of a series of mixed ligand ruthenium(II) complexes of the type $[Ru(pdto)(diimine)](ClO_4)_2$ **1–3** and $[Ru(bbdo)(diimine)](ClO_4)_2$ **4–6**, where pdto is 1,8-bis(pyrid-2-yl)-3,6-dithiooctane, bbdo is 1,8-bis(benzimidazol-2-yl)-3,6-dithiooctane and diimine is 1,10-phenanthroline (phen), dipyrido-[3,2-*d*:2′,3′-*f*]-quinoxaline (dpq) and dipyrido[3,2-*a*:2′,3′-*c*]phenazine (dppz) (Scheme 1). The rationale behind the design of these complexes is that the tetradentate ligands bis(pyrid-2-yl)-/bis(benzimidazol-2yl)-dithioether provide donor atoms such as imidazole nitrogen and thioether sulfur[19] to fine-tune the electronic properties and hence the DNA binding properties of octahedral Ru(II). The weakly π-accepting thioether and pyridine/benzimidazole (bzim) nitrogen donors have been shown to raise the redox potentials of Cu(II) and Ru(II) complexes significantly by stabilizing the lower oxidation states.[20] The primary ligand bbdo would be expected to form hydrogen bonds with suitable DNA functionalities to enhance the DNA binding. Also, biomolecules like proteins and nucleic acids[21a] containing such nitrogen donor atoms and sulfur-containing (bio)ligands are considered as potential partners in the bloodstream for binding to Ru(III) complexes,[21b,21c] which act as drugs by an activation-by-reduction mechanism.[5b] The co-ligands phen and extended 1,10-phenanthrolines with different numbers of aromatic rings to vary the surface area for intercalation would be expected to act as affinity ligands, and dictate the extent of DNA binding interaction of the complexes. The complexes are coordinatively saturated and rigid and so no covalent bonding is expected. Furthermore, among the present series of dicationic complexes, the electrostatic component of interaction does not change. The phen complexes **1a** and **4a** and the dpq complexes **2a** and **5** have been structurally characterized. The DNA binding of the Ru(II) complexes has been studied by using a variety of physical methods—absorption and emission spectroscopy, viscosity and electrochemical techniques. The ability of the complexes to unwind/untwist DNA has been studied by using supercoiled pBR322 DNA. The cytotoxicity of the dppz complexes **3** and **6**, which show stronger DNA binding affinities, has been studied by screening the complexes against cell lines of different cancer origins, *viz.* melanoma (A375), breast cancer (MDAMB-435 and MDAMB-468), glioblastoma (U373), fibrosarcoma (HT1080) and lung carcinoma (H460). It is remarkable that complex **6** exhibits a cytotoxicity higher than **3** towards all kinds of cell lines. Also, it displays higher cytotoxicity against melanoma than other cell lines and approximately twice the potency of cisplatin. An understanding of how the metal ion and ligand factors affect the biological activities should enable the design of metal complexes with specific medicinal properties.

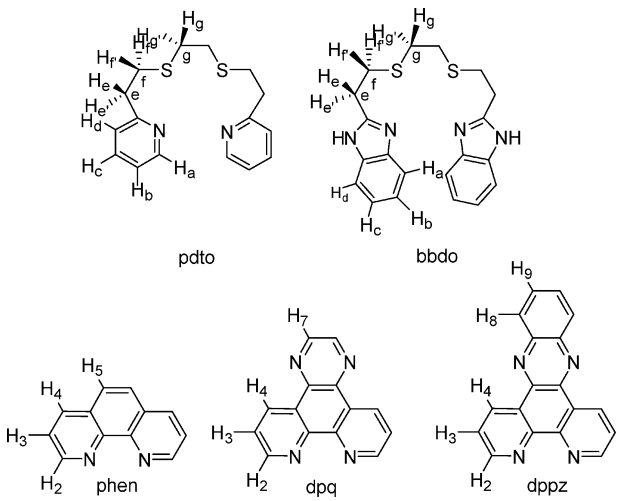


**Scheme 1** The structures and proton numbering schemes of ligands.

## Experimental

### Reagents and materials

$RuCl_3 \cdot 3H_2O$ (Arora Matthey), 2-vinylpyridine (Reilly), 3-chloropropionic acid, sodium borohydride (Fluka), 1,2-ethanedithiol and 1,10-phenanthroline (Aldrich), 1,2-diaminobenzene, ammonia solution (Loba Chemie), calf thymus (CT) DNA (highly

polymerized stored at 4 °C), superoxide dismutase (SOD, stored at: −20 °C), catalase (stored at: −20 °C), dimethyl sulfoxide (DMSO) and Hoechst 33258 (Sigma) and pBR322 supercoiled plasmid DNA (stored at: −20 °C) and agarose (Genei), adriamycin (Gensiasicor pharmaceuticals) and cisplatin (Bristol-Myers Squibb Co., Princeton) were used as received. Ultra-pure Milli-Q water (18.2 mΩ) was used in all experiments. The ligands dipyrido-[3,2-*d*:2′,3′-*f*]-quinoxaline (dpq)[22a] and dipyrido[3,2-*a*:2′,3′-*c*]phenazine (dppz)[22b] were prepared by reported procedures. Tetra-*n*-butylammonium perchlorate was prepared from tetra-*n*-butylammonium bromide (G. F. Smith) by using reported procedure[23] and recrystallized. Reagent grade solvents were dried and distilled by usual methods and the solvents were stored over molecular sieves (4 Å).

### Methods and instrumentation

Microanalysis (C, H and N) were carried out with a Vario EL elemental analyzer. An LCQ DECA XP electrospray mass spectrometer was employed for ESI-MS analysis. The solution electrical conductivity was obtained using a Systronic 305 conductivity bridge. UV-Vis spectroscopy was recorded on a Varian Cary 300 Bio UV-Vis spectrophotometer using cuvettes of 1 cm path length. Emission intensity measurements were carried out by using a Jasco F 6500 spectrofluorimeter. The $^1$H NMR spectra were obtained at room temperature using a Bruker 400 MHz spectrometer. The chemical shift values in DMSO-$d_6$ are reported with respect to tetramethylsilane as the internal standard and the values are reported as: $\delta$-values (multiplicity, assignment). Cyclic voltammetry and differential pulse voltammetry on a platinum sphere electrode were performed at 25 ± 0.2 °C. The temperature of the electrochemical cell was maintained by a cryocirculator (HAAKE D8-G). Voltammograms were generated with the use of an EG&G PAR Model 273 potentiostat. A Pentium IV computer along with EG&G M270 software was employed to control the experiments and acquire the data. A three-electrode system consisting of a platinum sphere (0.29 cm$^2$), a platinum auxiliary electrode and a reference electrode were used. The reference electrode for non-aqueous solution was Ag(s)/Ag$^+$, which consists of a Ag wire immersed in a solution of $AgNO_3$ (0.01 M) and tetra-*n*-butylammonium perchlorate (0.1 M) in acetonitrile placed in a tube fitted with a vycor plug using a sleeve.[24] The $E_{1/2}$ value observed under identical conditions for an Fc/Fc$^+$ couple in acetonitrile was 0.100 V with respect to the Ag/Ag$^+$ reference electrode. The cyclic voltammograms (CV) and differential pulse voltammograms (DPV) of **1–6** were obtained in MeCN solutions with 0.1 M $[(C_4H_9)_4N]ClO_4$ as the supporting electrolyte at ambient temperatures under $N_2$. Redox potentials were measured relative to a Ag/Ag$^+$ reference electrode. All the complexes are electroactive with respect to the metal as well as the ligand centers in the potential range ±2 V.

Solutions of DNA in the buffer 5 mM Tris-HCl/50 mM NaCl (pH = 7.1) in water gave the ratio of UV absorbance at 260 and 280 nm, $A_{260}/A_{280}$, of 1.9, indicating that the DNA was sufficiently free of protein.[25] Concentrated stock solutions of DNA (10.5 mM) were prepared in a buffer and sonicated for 25 cycles, where each cycle consisted of 30 s with 1 min intervals. The concentration of DNA in nucleotide phosphate (NP) was determined by UV absorbance at 260 nm after 1 : 100 dilutions. The extinction coefficient, $\varepsilon_{260}$, was taken as 6600 M$^{-1}$ cm$^{-1}$. Stock solutions were stored at 4 °C and used after no more than 4 d. Supercoiled plasmid pBR322 DNA was stored at: −20 °C and the concentration of DNA in base pairs was determined by UV absorbance at 260 nm after appropriate dilutions taking $\varepsilon_{260}$ as 13 100 M$^{-1}$ cm$^{-1}$. Concentrated stock solutions of metal complexes were prepared by dissolving calculated amounts of ruthenium complexes in respective amounts of solvent and diluted suitably with the corresponding buffer to required concentrations for all experiments.

### Synthesis of ligands

The ligands 1,8-bis(pyrid-2-yl)-3,6-dithiaoctane[26] (pdto) and 1,8-bis(benzimidazol-2-yl)-3,6-dithiaoctane[27] (bbdo) were prepared according to the reported procedures.

### Synthesis of ruthenium(II) complexes

**CAUTION!** *During handling of the perchlorate salts of metal complexes with organic ligands care should be taken because of the possibility of explosion.*

**[Ru(pdto)Cl]$_2$(ClO$_4$)$_2$ and [Ru(bbdo)Cl]$_2$(ClO$_4$)$_2$.** The di-μ-chloro dimers were synthesized according to the published procedure.[20a]

**[Ru(pdto)(phen)](ClO$_4$)$_2$ (1) and [Ru(pdto)(phen)](PF$_6$)$_2$·CH$_3$OH·2H$_2$O (1a).** The compound [Ru(pdto)Cl]$_2$(ClO$_4$)$_2$ (0.27 g, 0.25 mmol) dissolved in hot ethanol (50 mL) was added to phen (0.09 g, 0.5 mmol) in ethanol (25 mL). The mixture was heated to continuous reflux for 12 h. The yellowish orange solution was cooled to room temperature and rotaevaporated to 10 mL. The crude product was precipitated by adding aqueous $NaClO_4$/$KPF_6$. The resultant yellow–orange precipitate was filtered off, washed with ether and dried *in vacuo*. Yield, 0.31 g, 79%. Anal. Calc. for $C_{28}H_{28}N_4S_2Cl_2O_8Ru$: C, 42.86, H, 3.60, N, 7.14. Found: C, 42.55, H, 3.82, N, 7.26%. $\Lambda_M$, 300 Ω$^{-1}$ cm$^2$ mol$^{-1}$. Electronic absorption spectrum in MeCN [$\lambda$/nm ($\varepsilon$/M$^{-1}$ cm$^{-1}$)]: 250 (18 110), 270 (23 720), 300 (9030), 330 (6960), 400 (5220), 435 (sh, 5050). The chloride salt was prepared from their $ClO_4$/$PF_6$ salts by precipitating it from an acetone solution of the $ClO_4$/$PF_6$ salt with tetra-*n*-butylammonium chloride. Yellow orange crystals of **1a** suitable for X-ray diffraction studies were obtained by dissolving the complex **1** in 10 mL MeCN–MeOH (1 : 1 v/v, 5 mL each), adding saturated aqueous solution of $KPF_6$ (2 mL) and allowing the solution to evaporate slowly at room temperature over 15 d.

**[Ru(pdto)(dpq)](ClO$_4$)$_2$ (2).** This compound was prepared by refluxing [Ru(pdto)Cl]$_2$(ClO$_4$)$_2$ (0.27 g, 0.25 mmol) and dpq (0.09 g, 0.5 mmol) in ethanol (50 mL) for 12 h using the procedure employed for **1**. Yield, 0.35 g, 80%. Anal. Calc. for $C_{30}H_{28}N_6S_2Cl_2O_8Ru$: C, 43.07, H, 3.37, N, 10.04%. Found: C, 42.96, H, 3.60, N, 10.14. $\Lambda_M$, 306 Ω$^{-1}$ cm$^2$ mol$^{-1}$. Electronic absorption spectrum in MeCN [$\lambda$/nm ($\varepsilon$/M$^{-1}$ cm$^{-1}$)]: 260 (75 942), 295 (26 677), 324 (14 729), 431 (6197). ESI-MS: [Ru(pdto)(dpq)]$^{2+}$ displays peak at $m/z$ = 318.00, calculated = 318.94. The chloride salt was prepared from the $ClO_4$ salt by precipitating it from an acetone solution of the $ClO_4$ salt with tetra-*n*-butylammonium chloride.

 

**[Ru(pdto)(dpq)(Cl)](PF$_6$) (2a).** This compound was prepared by refluxing [Ru(pdto)Cl]$_2$(ClO$_4$)$_2$ (0.27 g, 0.25 mmol) and dpq (0.09 g, 0.5 mmol) in ethanol (50 mL) for 12 h using the procedure employed for **1**. This compound was isolated as yellow–orange crystals suitable for X-ray diffraction studies by dissolving the corresponding PF$_6$ salt in 10% DMF–5 mM Tris-HCl–50 mM NaCl buffer at pH 7.1 and then allowing the solution to evaporate slowly at room temperature for several days.

**[Ru(pdto)(dppz)](ClO$_4$)$_2$ (3) and [Ru(pdto)(dppz)](PF$_6$)$_2$ (3a).** This compound was prepared by refluxing [Ru(pdto)Cl]$_2$(ClO$_4$)$_2$ (0.27 g, 0.25 mmol) and dppz (0.14 g, 0.5 mmol) in ethanol (50 mL) for 12 h using the procedure employed for **1**. Yield, 0.31 g, 70%. Anal. Calc. for $C_{34}H_{30}N_6S_2Cl_2O_8Ru$: C, 46.05; H, 3.41; N, 9.48. Found: C, 46.11; H, 3.62; N, 9.59%. $\Lambda_M$, 301 $\Omega^{-1}$ cm$^2$ mol$^{-1}$. Electronic absorption spectrum in MeCN [$\lambda$/nm ($\varepsilon$/M$^{-1}$ cm$^{-1}$)]: 270 (28 570), 360 (15 100), 440 (7380). The chloride salt was prepared from their ClO$_4$/PF$_6$ salts by precipitating it from an acetone solution of the ClO$_4$/PF$_6$ salt with tetra-*n*-butylammonium chloride.

**[Ru(bbdo)(phen)](ClO$_4$)$_2$ (4) and [Ru(bbdo)(phen)](PF$_6$)$_2$·CH$_3$CN·H$_2$O (4a).** This compound was prepared by refluxing [Ru(bbdo)Cl]$_2$(ClO$_4$)$_2$ (0.31 g, 0.25 mmol) and phen (0.09 g, 0.5 mmol) in ethanol (50 mL) for 12 h using the procedure employed for **1**. Yield, 0.32 g, 74%. Anal. Calc. for $C_{32}H_{30}N_6S_2Cl_2O_8Ru$: C, 44.55; H, 3.50; N, 9.74. Found: C, 44.11; H, 3.62; N, 9.59%. $\Lambda_M$, 298 $\Omega^{-1}$ cm$^2$ mol$^{-1}$. Electronic absorption spectrum in MeCN [$\lambda$/nm ($\varepsilon$/M$^{-1}$ cm$^{-1}$)]: 270 (30 090), 330 (5680), 415 (sh, 3100), 455 (3150). The chloride salt was prepared from their ClO$_4$/PF$_6$ salts by precipitating it from an acetone solution of the ClO$_4$/PF$_6$ salt with tetra-*n*-butylammonium chloride. Yellow–orange crystals of **4a** suitable for X-ray diffraction studies were obtained by dissolving the complex **4** in 10 mL MeCN–MeOH (1 : 1 v/v, 5 mL each), adding saturated aqueous solution of KPF$_6$ (2 mL) and then allowing the solution to evaporate slowly at room temperature for 18 d.

**[Ru(bbdo)(dpq)](ClO$_4$)$_2$ (5) and [Ru(bbdo)(dpq)](PF$_6$)$_2$ (5a).** This compound was prepared by refluxing [Ru(bbdo)Cl]$_2$(ClO$_4$)$_2$ (0.31 g, 0.25 mmol) and dpq (0.14 g, 0.5 mmol) in ethanol for 12 h using the procedure employed for **1**. Yield, 0.34 g, 71%. Anal. Calc. for $C_{34}H_{30}N_8S_2Cl_2O_8Ru$: C, 44.64; H, 3.31; N, 12.25. Found: C, 44.39; H, 3.59; N, 12.52%. $\Lambda_M$, 302 $\Omega^{-1}$ cm$^2$ mol$^{-1}$. Electronic absorption spectrum in MeCN [$\lambda$/nm ($\varepsilon$/M$^{-1}$ cm$^{-1}$)]: 258 (39 854), 294 (17 861), 461 (3078). The chloride salt was prepared from their ClO$_4$/PF$_6$ salts by precipitating it from an acetone solution of the ClO$_4$/PF$_6$ salt with tetra-*n*-butylammonium chloride. The red–orange solid was recrystallized from acetonitrile–methanol–ether mixture.

**[Ru(bbdo)(dppz)](ClO$_4$)$_2$ (6) and [Ru(bbdo)(dppz)](PF$_6$)$_2$ (6a).** This compound was prepared by refluxing [Ru(bbdo)Cl]$_2$(ClO$_4$)$_2$ (0.31 g, 0.25 mmol) and dppz (0.14 g, 0.5 mmol) in ethanol (50 mL). Yield, 0.34 g, 71%. Anal. Calc. for $C_{38}H_{32}N_8S_2Cl_2O_8Ru$: C, 47.31; H, 3.34; N, 11.61. Found: C, 47.09; H, 3.59; N, 11.52%. $\Lambda_M$, 300 $\Omega^{-1}$ cm$^2$ mol$^{-1}$. Electronic absorption spectrum in MeCN [$\lambda$/nm ($\varepsilon$/M$^{-1}$cm$^{-1}$)]: 280 (32 125), 330 (10 020), 375 (8660), 465 (3210). The chloride salt was prepared from their ClO$_4$/PF$_6$ salts by precipitating it from an acetone solution of the ClO$_4$/PF$_6$ salt with tetra-*n*-butylammonium chloride.

### X-Ray crystallography†

Crystals of **1a** and **4a** showing nice extinction under a polarizing microscope were used for data collection with a Enraf-Noinus-CAD4 diffractometer attached to a CCD area detector using Mo-K$\alpha$ radiation. The $\omega$-2$\theta$ scan technique was used to record the intensity data. The unit cell parameters and the orientation matrix of the crystals were determined by least-square treatment of 25 reflections. A hemisphere of reciprocal space was then collected using SMART software[28] with the 2$\theta$ setting at 28°. The data reduction involved Lorentz- and polarization effects and an empirical absorption correction based on $\omega$-scan reflections were applied using the MolEN program.[29] The structure of crystals were solved by the Patterson method using SHELXS 97 and refined by full matrix least-squares method on $F^2$ using SHELXL 97.[30] All the non-hydrogen atoms were refined anisotropically. Hydrogen atoms were geometrically fixed at their calculated positions. The crystallographic data and details of data collection for **1a** and **4a** are given in Table 1. Graphical representations of the structure were made with POV-Ray v3.6.[31] In the case of complex **1a**, after complete refinement of the complex cation and PF$_6$ anions, closely associated diffuse peaks with electron density varying from 3.2 Å$^{-3}$ to 2.0 Å $^{-3}$ appeared in the difference Fourier map, which are assigned as disordered water molecules, and are included in the refinement isotropically with occupancy factor depending on the peak height.

The crystals of **2a** and **5** of suitable size were selected from the mother liquor and immersed in partone oil, then mounted on the tip of a glass fiber and cemented using epoxy resin. Intensity data for all three crystals were collected using Mo-K$\alpha$ ($\lambda$ = 0.71073 Å) radiation on a Bruker SMART APEX diffractometer equipped with CCD area detector at 100 K. The data integration and reduction were processed with SAINT[32] software. An empirical absorption correction was applied to the collected reflections with SADABS.[33] The structures were solved by direct methods using SHELXTL[34] and were refined on $F^2$ by the full-matrix least-squares technique using the SHELXL-97[30] program package. In both the compounds all non-hydrogen atoms were refined anisotropically till convergence is reached. Hydrogen atoms attached to the ligand moieties are stereochemically fixed. The crystallographic data and details of data collection for **2a** and **5** are given in Table 1. Graphical representations of the structure were made with POV-Ray v3.6.[31]

### DNA binding experiments

Concentrated stock solutions of metal complexes were prepared by dissolving them in a 10% DMF–5 mM Tris-HCl–50 mM NaCl buffer (0.5 mL of DMF in 5 mL of buffer) at pH 7.1 and diluting suitably with the corresponding buffer to required concentrations for all the experiments. For absorption and emission spectral experiments the DNA solutions were pretreated with the solutions of metal complexes to ensure no change in the metal complex concentrations. The absorption spectra were recorded on a Varian Cary 300 Bio UV-Vis spectrophotometer using cuvettes of 1 cm path length.

Absorption spectral titration experiments were performed by maintaining a constant concentration of the complex and varying the nucleic acid concentration. This was achieved by dissolving

**Table 1** Selected crystallographic data for the complexes **1a**, **2a**, **4a** and **5**

| | **1a** | **2a** | **4a** | **5** |
|---|---|---|---|---|
| Empirical formula | $C_{28}H_{28}F_{12}N_4O_3P_2S_2Ru$ | $C_{30}H_{28}F_6ClN_6PS_2Ru$ | $C_{34}H_{35}F_{12}N_7OP_2S_2Ru$ | $C_{34}H_{30}Cl_2N_8O_8S_2Ru$ |
| $M$ | 923.67 | 818.21 | 1012.82 | 914.77 |
| Crystal system | Triclinic | Monoclinic | Monoclinic | Orthorhombic |
| Space group | $P\bar{1}$ | $P2_1/c$ | $P2_1/a$ | $Pnna$ |
| $a$/Å | 11.0191(16) | 14.9570(13) | 14.886(4) | 29.804(7) |
| $b$/Å | 11.9487(15) | 9.0588(8) | 18.276(8) | 14.946(4) |
| $c$/Å | 15.368(4) | 23.1298(19) | 16.665(4) | 15.875(4) |
| $\alpha$/° | 69.991(14) | 90.000 | 90.000 | 90.000 |
| $\beta$/° | 87.531(17) | 100.962(2) | 115.44(2) | 90.000 |
| $\gamma$/° | 73.954(12) | 90.000 | 90.000 | 90.000 |
| $V$/Å | 1824.3(6) | 3076.7(5) | 4094(2) | 7072(3) |
| $Z$ | 2 | 4 | 4 | 8 |
| $\rho_{calcd}$/g cm$^{-3}$ | 1.682 | 1.766 | 1.643 | 1.718 |
| μ/cm$^{-1}$ | 7.30 | 8.6 | 6.57 | 7.8 |
| $\lambda$(Mo-Kα)/Å | 0.71073 | 0.71073 | 0.71073 | 0.71073 |
| $T$/K | 293(2) | 100(2) | 293(2) | 100(2) |
| $F$(000) | 924 | 1648 | 2040 | 3712 |
| Reflections collected | 6841 | 18 125 | 6720 | 26 753 |
| Independent reflections | 6402 | 7198 | 6422 | 4636 |
| $R_{int}$ | 0.0261 | 0.0659 | 0.0524 | 0.2012 |
| Goodness-of-fit on $F^2$ | 1.1617 | 1.223 | 1.138 | 1.016 |
| $R^a$ | 0.0533 | 0.0745 | 0.0716 | 0.0716 |
| $R_w{}^b$ | 0.1464 | 0.1587 | 0.1690 | 0.1349 |

$^a$ $R = \Sigma \| F_o | - | F_c \| / \Sigma | F_o |$. $^b$ $R_w = [\Sigma w(|F_o| - |F_c|)^2 / \Sigma w |F_o|^2]^{1/2}$.

an appropriate amount of the metal complex and DNA stock solutions while maintaining the total volume constant (1 mL). This results in a series of solutions with varying concentrations of DNA but with a constant concentration of the complex. The absorbance (A) was recorded after successive additions of CT DNA. Fits of experimental absorption titrations were performed with Mathematica v3.

Emission intensity measurements were carried out using Jasco F 6500 spectrofluorimeter. The tris buffer was used as a blank to make preliminary adjustments. The excitation wavelength was fixed and the emission range was adjusted before measurements. DNA was pretreated with ethidium bromide in the ratio [NP]/[EthBr] = 10 for 30 min at 27 °C. The metal complexes (0–60 μM) were then added to this mixture and their effect on the emission intensity was measured. Competitive binding experiment with Hoechst 33258, a minor groove binder, has been carried out following the procedure as suggested for EthBr experiments. For viscosity measurements a Schott Gerate AVS 310 automated viscometer was thermostated at 25 ± 1 °C in a constant temperature bath. DNA concentration was kept constant (200 μM in NP) and the concentration of metal complexes varied ($1/R$ = [Ru]/[DNA] = 0.0–0.50). The flow times were noted from the digital timer attached with the viscometer. Data are presented as $\eta/\eta_0$ *vs.* $1/R$, where $\eta$ is the viscosity of DNA in the presence of the ruthenium(II) complex and $\eta_0$ is the relative viscosity of DNA alone. Relative viscosity values were calculated from the observed flow time of the DNA solution ($t$) corrected for the flow time of the buffer alone ($t_0$), using the expression $\eta_0 = (t - t_0)/t_0$.

All the cyclic (CV) and differential pulse voltammetry (DPV) experiments were performed in a single compartment cell with a three electrode configuration on an EG&G PAR 273 potentiostat/galvanostat equipped with P IV computer. Freshly-cleaned indium tin oxide (ITO) was the working electrode, and the reference was a saturated calomel electrode. A platinum plate was used as the counter electrode. The supporting electrolyte was a 50 mM NaCl–5 mM Tris HCl buffer at pH 7.1. Solutions were deoxygenated by purging with $N_2$ gas for 15 min prior to the measurements and during the measurements a stream of $N_2$ gas was passed over the solution. All measurements were carried out at 25.0 ± 0.2 °C, maintained by a HAAKE D8-G circulating bath. The redox potential $E_{1/2}$ was calculated from the anodic ($E_{pa}$) and cathodic ($E_{pc}$) peak potentials of CV traces as $(E_{pa} + E_{pc})/2$ and also from the peak potential ($E_{pa}$) of DPV response as $E_p + \Delta E/2$ ($\Delta E$ is the pulse height).

The interaction of complexes with supercoiled pBR322 DNA was monitored using agarose gel electrophoresis. In reactions using supercoiled pBR322 plasmid DNA (Form I, 40 μM) in a 10% DMF–5 mM Tris-HCl–50 mM NaCl buffer at pH 7.1 was treated with metal complexes in the same buffer. For photocleavage studies, the reactions were carried out under illuminated conditions at 365 nm (12 W) monochromatic light source. In each experiment supercoiled pBR322 DNA (Form I, 40 μM) was treated with metal complexes (60 μM) and irradiated at 365 nm monochromatic wavelength for 5 min. The samples were then incubated for 1 h in the dark for 37 °C and analysed for the photocleaved products using gel electrophoresis as discussed below. A loading buffer containing 25% bromophenol blue, 0.25% xylene cyanol and 30% glycerol (3 μl) was added and electrophoresis performed at 60 V for 5 h in Tris–Acetate–EDTA (TAE) buffer (40 mM Tris base, 20 mM acetic acid, 1 mM EDTA) using 1% agarose gel containing 1.0 μg mL$^{-1}$ ethidium bromide.[35] The gels were viewed in a Gel doc system and photographed using a CCD camera (Alpha Innotech Corporation). For anaerobic experiments deoxygenated water and anaerobic stock solutions were prepared by purging with $N_2$. In order to identify the reactive oxygen species (ROS) involved in the cleavage reaction the radical scavengers such as hydroxyl radical

 

(DMSO, 10%), singlet oxygen ($NaN_3$, 100 μM), superoxide (SOD, 10 unit) and $H_2O_2$ (catalase, 0.1 unit) were introduced.

### Cell lines and culture conditions

Human cancer cell lines A375 (melanoma), U373 (glioblastoma), HT1080 (fibrosarcoma) and H460 (lung carcinoma) were described previously.[36,37] MDAMB-435 (ductal carcinoma), MDAMB-468 (breast cancer) and human immortalized keratinocytes (HaCaT) were grown in DMEM (Sigma) supplemented with 10% FCS (Sigma). All the cell lines were maintained in a $CO_2$ incubator at 37 °C and 5% $CO_2$.

### MTT assay

MTT assay was carried out as described previously.[38] The cells were plated in 96-well plates with cell numbers ranging between 500 and 4000 cells per well for different cell lines. After 24 h of plating, the cells were treated with complex **3** or **6**, adriamycin and cisplatin. MTT (20 μL of 5 mg $mL^{-1}$) was added 48 h after infection. MTT is a tetrazolium salt that is converted by living cells into blue formazan crystals. The medium was removed from the wells 3 h after MTT addition and 200 μL of DMSO was added to dissolve the formazan crystals and then the absorbance was measured at 550 nm in an ELISA reader. The concentrations of the stock solutions of the different compounds used were: adriamycin (3.5 mM), cisplatin (3.3 mM), complexes **3** and **6** (10 mM). The stock solutions of the metal complexes were prepared in DMSO and in all the experiments the percentage of DMSO was maintained in the range of 0.1–1%. DMSO by itself was found to be non-toxic to the cells till 1% concentration.

## Results and discussion

### Synthesis of ruthenium(II) complexes

The mixed ligand complexes [Ru(pdto)(phen)]$(ClO_4)_2$ **1**, [Ru(pdto)(dpq)]$(ClO_4)_2$ **2**, [Ru(pdto)(dppz)]$(ClO_4)_2$ **3**, [Ru(bbdo)(phen)]$(ClO_4)_2$ **4**, [Ru(bbdo)(dpq)]$(ClO_4)_2$ **5** and [Ru(bbdo)(dppz)]$(ClO_4)_2$ **6**, where pdto = 1,8-bis(pyrid-2-yl)-3,6-dithiooctane, bbdo = 1,8-bis(benzimidazol-2-yl)-3,6-dithiooctane and phen = 1,10-phenanthroline, dpq = dipyrido-[3,2-*d*:2′,3′-*f*]-quinoxaline and dppz = dipyrido[3,2-*a*:2′,3′-*c*]phenazine, have been isolated by reacting the dinuclear complexes[20a] [Ru(pdto)(μ-Cl)]$_2(ClO_4)_2$ and [Ru(bbdo)(μ-Cl)]$_2(ClO_4)_2$ with the corresponding diimine ligands. They were also isolated as the $PF_6^-$ salts. The elemental analyses of the complexes were consistent with the formula [Ru(L)(diimine)]$X_2$, where L = pdto or bbdo and diimine = phen or dpq or dppz and X = $ClO_4$. Two alternative stereoisomers, namely, "*cis*-α" and "*cis*-β" are possible for the octahedral Ru(II) complexes of linear tetradentate $N_2S_2$ ligands (Scheme 2).[20a] In addition, each of these stereoisomers is chiral and therefore can exist in either a left-handed (Λ) or right-handed (Δ) enantiomeric form. Interestingly, the X-ray crystal structures of the complexes possess predominantly the "*cis*-α" configuration in which the $N_2S_2$ ligands are folded. A very strong and broad band near 1100 $cm^{-1}$ and a strong and sharp band near 620 $cm^{-1}$ are observed in the IR spectra of the complexes, which is in agreement with the presence of uncoordinated ionic perchlorate in their crystal structures. Thus the complexes act as

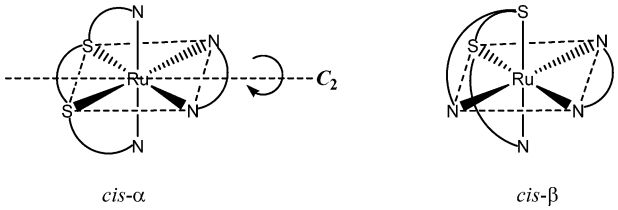


*cis*-α *cis*-β

**Scheme 2** Representations of "*cis*-α" (left) and "*cis*-β" (right) isomeric forms of [Ru(pdto/bbdo)(diimine)]$^{2+}$ cations. The α-form possesses a $C_2$ symmetry as indicated whilst the β-form is asymmetric.

1 : 2 electrolytes in acetonitrile solution. The chloride salt was prepared from their $ClO_4^-$ or $PF_6^-$ salt by precipitating it from an acetone solution of the $ClO_4^-$ or $PF_6^-$ salt with the addition of tetra-*n*-butylammonium chloride. The complexes are soluble in both polar and non-polar solvents. The chloride salts of **1–3** are highly soluble in water but those of **4–6** are soluble in a 10% DMF–5 mM Tris-HCl–50 mM NaCl buffer at pH 7.1. So solutions of the complexes were prepared in a 10% DMF–5 mM Tris-HCl–50 mM NaCl buffer at pH 7.1 for DNA binding studies.

**Description of structures of [Ru(pdto)(phen)]$(PF_6)_2\cdot CH_3OH\cdot 2H_2O$ (1a), [Ru(bbdo)(phen)]$(PF_6)_2\cdot CH_3CN\cdot H_2O$ (4a) and [Ru(bbdo)(dpq)]$(ClO_4)_2$ (5).** The ball-and-stick representation of the crystal structures of [Ru(pdto)(phen)]$(PF_6)_2\cdot CH_3OH\cdot 2H_2O$ **1a**, [Ru(bbdo)(phen)]$(PF_6)_2\cdot CH_3CN\cdot H_2O$ **4a** and [Ru(bbdo)(dpq)]$(ClO_4)_2$ **5** are illustrated in Fig. 1–3 respectively with atom numbering scheme. The selected bond lengths and bond angles are given in Table 2. The complexes **1a**, **4a** and **5** possess distorted octahedral coordination geometries, as evident from the bond angles, which deviate from the ideal bond angles of 90° and 180°. The tetradentate ligands pdto and bbdo are folded around Ru(II) to form exclusively the "*cis*-α" rather than "*cis*-β" isomer due to *cis*-coordination of bidentate phen and dpq ligands. We have already shown that the *cis*-α configuration is exhibited by the analogous [Ru(pdto)(bpy)]$^{2+}$ and [Ru(bbdo)(bpy)]$^{2+}$ complexes.[20a]

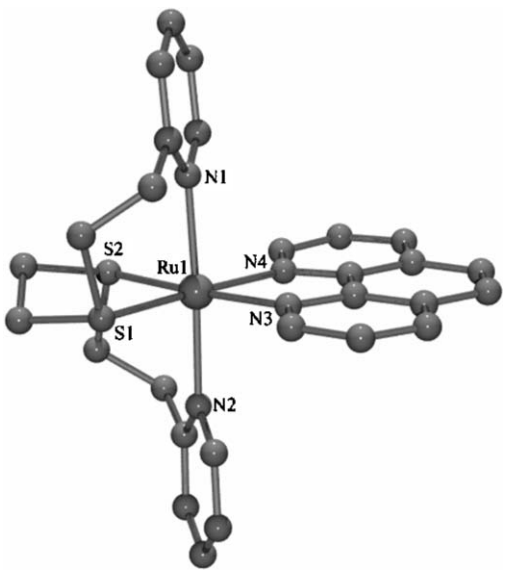


**Fig. 1** Ball-and-stick representation of the crystal structure of [Ru(pdto)(phen)]$^{2+}$ cation **1a**; atoms as spheres of arbitrary diameter. Hydrogen atoms are omitted for clarity.

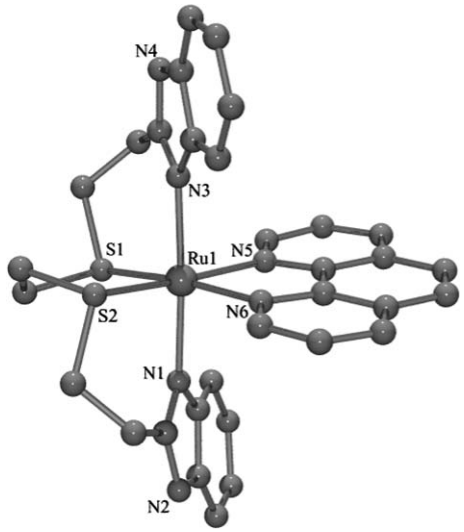


**Fig. 2** Ball-and-stick representation of the crystal structure of $[Ru(bbdo)(phen)]^{2+}$ cation **4a**; atoms as spheres of arbitrary diameter. Hydrogen atoms are omitted for clarity.

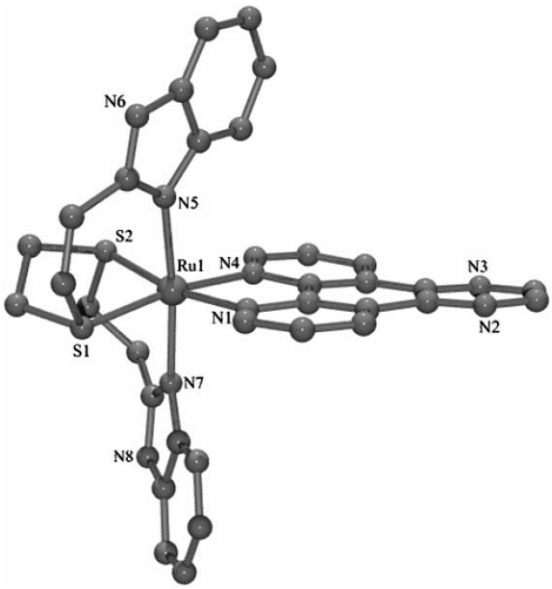


**Fig. 3** Ball-and-stick representation of the crystal structure of $[Ru(bbdo)(dpq)]^{2+}$ cation **5**; atoms as spheres of arbitary diameter. Hydrogen atoms are omitted for clarity.

The Ru–S distances observed in **1a** (2.3117(14), 2.3025(13) Å), **4a** (2.307(3), 2.324(3) Å) and **5** (2.304(3), 2.313(3) Å) fall within the range 2.19–2.59 Å observed for other Ru(II) complexes[39,40] of thioether ligands. The Ru–$N_{py}$ (**1a**, 2.140(4), 2.153(4) Å), Ru–$N_{bzim}$ (**4a**, 2.110(7), 2.138(8); **5**, 2.160(8), 2.141(8) Å), Ru–$N_{phen}$ (**1a**, 2.105(3), 2.123(4); **4a**, 2.103(7), 2.126(8) Å) and Ru–$N_{dpq}$ (**5**, 2.092(9), 2.095(6) Å) bond lengths are normal.[41,42] The average Ru–$N_{phen}$ bond length in **4a** (2.114 Å) is similar to that in **1a** (2.115 Å). The planarity of the phen residue in **1a** and **4a** is manifested chiefly in the almost identical S–Ru–S bite angles (**1a**, 87.4(4); **4a**, 87.6(11)°). As expected, the Ru–$N_{phen}$ and Ru–$N_{dpq}$ bond distances are significantly shorter than the Ru–$N_{py}$ or Ru–$N_{bzim}$ bond distances reflecting the strong π-back bonding involving

**Table 2** Selected interatomic distances (Å) and angles (°) for complexes **1a**, **2a**, **4a** and **5**

$[Ru(pdto)(phen)](PF_6)_2 \cdot CH_3OH \cdot 2H_2O$ **1a**

| | | | |
|---|---|---|---|
| Ru(1)–N(3) | 2.123(4) | Ru(1)–N(4) | 2.105(3) |
| Ru(1)–N(2) | 2.140(4) | Ru(1)–N(1) | 2.153(4) |
| Ru(1)–S(2) | 2.3025(13) | Ru(1)–S(1) | 2.3117(14) |
| N(3)–Ru(1)–N(4) | 78.54(14) | N(3)–Ru(1)–N(2) | 93.20(13) |
| N(4)–Ru(1)–N(2) | 88.89(13) | N(3)–Ru(1)–N(1) | 88.72(12) |
| N(4)–Ru(1)–N(1) | 93.77(12) | N(2)–Ru(1)–N(1) | 176.99(12) |
| N(3)–Ru(1)–S(2) | 96.72(9) | N(4)–Ru(1)–S(2) | 175.04(9) |
| N(2)–Ru(1)–S(2) | 92.52(10) | N(1)–Ru(1)–S(2) | 84.94(9) |
| N(3)–Ru(1)–S(1) | 175.85(9) | N(4)–Ru(1)–S(1) | 97.43(10) |
| N(2)–Ru(1)–S(1) | 86.09(10) | N(1)–Ru(1)–S(1) | 92.16(9) |
| S(2)–Ru(1)–S(1) | 87.41(4) | | |

$[Ru(pdto)(dpq)(Cl)](PF_6)$ **2a**

| | | | |
|---|---|---|---|
| Ru(1)–Cl(1) | 2.4292(14) | Ru(1)–N(1) | 2.074(5) |
| Ru(1)–S(1) | 2.3096(15) | Ru(1)–N(2) | 2.113(4) |
| Ru(1)–S(2) | 2.3300(15) | Ru(1)–N(5) | 2.130(5) |
| Cl(1)–Ru(1)–S(1) | 90.67(5) | S(1)–Ru(1)–N(5) | 91.02(13) |
| Cl(1)–Ru(1)–S(2) | 178.31(5) | S(2)–Ru(1)–N(1) | 91.79(13) |
| Cl(1)–Ru(1)–N(1) | 88.47(13) | S(2)–Ru(1)–N(2) | 98.11(13) |
| Cl(1)–Ru(1)–N(2) | 83.58(13) | S(2)–Ru(1)–N(5) | 85.82(13) |
| Cl(1)–Ru(1)–N(5) | 94.07(13) | N(1)–Ru(1)–N(2) | 78.91(18) |
| S(1)–Ru(1)–S(2) | 87.64(5) | N(1)–Ru(1)–N(5) | 174.40(18) |
| S(1)–Ru(1)–N(1) | 93.95(13) | N(2)–Ru(1)–N(5) | 96.40(17) |
| S(1)–Ru(1)–N(2) | 170.91(13) | | |

$[Ru(bbdo)(phen)](PF_6)_2 \cdot CH_3CN \cdot H_2O$ **4a**

| | | | |
|---|---|---|---|
| Ru(1)–N(6) | 2.103(7) | Ru(1)–N(1) | 2.110(7) |
| Ru(1)–N(5) | 2.126(8) | Ru(1)–N(3) | 2.138(8) |
| Ru(1)–S(2) | 2.307(3) | Ru(1)–S(1) | 2.324(3) |
| N(6)–Ru(1)–N(1) | 88.4(3) | N(6)–Ru(1)–N(5) | 78.4(3) |
| N(1)–Ru(1)–N(5) | 94.1(3) | N(6)–Ru(1)–N(3) | 94.7(3) |
| N(1)–Ru(1)–N(3) | 176.7(3) | N(5)–Ru(1)–N(3) | 87.8(3) |
| N(6)–Ru(1)–S(2) | 95.5(2) | N(1)–Ru(1)–S(2) | 90.9(2) |
| N(5)–Ru(1)–S(2) | 171.9(2) | N(3)–Ru(1)–S(2) | 87.5(2) |
| N(6)–Ru(1)–S(1) | 172.7(2) | N(1)–Ru(1)–S(1) | 85.0(2) |
| N(5)–Ru(1)–S(1) | 99.1(2) | N(3)–Ru(1)–S(1) | 92.1(2) |
| S(2)–Ru(1)–S(1) | 87.6(11) | | |

$[Ru(bbdo)(dpq)](ClO_4)_2$ **5**

| | | | |
|---|---|---|---|
| Ru(1)–S(1) | 2.313(3) | Ru(1)–N(4) | 2.095(6) |
| Ru(1)–S(2) | 2.304(3) | Ru(1)–N(5) | 2.160(8) |
| Ru(1)–N(1) | 2.092(9) | Ru(1)–N(7) | 2.141(8) |
| S(1)–Ru(1)–S(2) | 87.6(11) | S(2)–Ru(1)–N(7) | 93.0(2) |
| S(1)–Ru(1)–N(1) | 101.7(2) | N(1)–Ru(1)–N(4) | 77.9(3) |
| S(1)–Ru(1)–N(4) | 170.1(2) | N(1)–Ru(1)–N(5) | 86.5(3) |
| S(1)–Ru(1)–N(5) | 91.1(2) | N(1)–Ru(1)–N(7) | 95.1(3) |
| S(1)–Ru(1)–N(7) | 82.4(2) | N(4)–Ru(1)–N(5) | 98.8(3) |
| S(2)–Ru(1)–N(1) | 168.3(2) | N(4)–Ru(1)–N(7) | 87.8(3) |
| S(2)–Ru(1)–N(4) | 94.1(3) | N(5)–Ru(1)–N(7) | 173.5(3) |
| S(2)–Ru(1)–N(5) | 86.4(2) | | |

the extensively delocalized[43] π-molecular orbitals of phen/dpq ligands and Ru(II) $t_2$ orbitals. Also, the bzim nitrogens (**4a**, **5**) are involved in σ-bonding more strongly than the py nitrogen (**1**), as evident from the shorter Ru–$N_{bzim}$ distances compared to Ru–$N_{py}$ distances. The phen ligands are planar with the Ru atom being only 0.024 (**1a**) and 0.030 Å (**4a**) out of the $C_{12}N_2$ plane

 

in the chelate ring involving phen and the near planarity of the diimine ligands are expected to make these complexes potential DNA intercalators.

**Description of structure of [Ru(pdto)(dpq)(Cl)](PF$_6$) (2a).** The ball-and-stick representation of the crystal structure of **2a** is illustrated in Fig. 4 with atom numbering scheme. The selected bond lengths and bond angles are given in Table 2. The complex cation possesses a distorted octahedral coordination geometry as evident from the bond angles, which deviate from the ideal values of 90° and 180°. In contrast to **1a** the pdto ligand in **2a** acts as a tridentate ligand with one of its coordinated pyridine nitrogens replaced by a chloride ion. One of the sulfur atoms occupies a position *trans* to the chloride ion. The observed Ru–S bond distances in **2a** (Ru–S1, 2.3096(15); Ru–S2, 2.3300(15) Å) fall within the range for Ru–S(thioether) bond lengths (2.19–2.59 Å)[43–46] with an average value of 2.320 Å in Ru(II) complexes. As expected, the two Ru–S bond distances are only slightly different implying that fusion of a benzene ring to phen as in dpq has only a small influence on the π–delocalization of electrons. The average Ru–$N_{py}$ and Ru–$N_{dpq}$ bond lengths are normal and fall within the range of 2.00–2.13 Å observed in other Ru(II) polypyridyl complexes.[41,42] Furthermore, the Ru–$N_{py}$ bond lengths [Ru–N5, 2.130(5) Å] in **2a** are significantly longer than the Ru–$N_{dpq}$ bond lengths [Ru–N1, 2.074(5); Ru–N2(4), 2.113(4) Å], which is expected of the stronger π-back bonding of the extended phen ring of dpq compared to the py ring. The Ru–Cl bond length [Ru–Cl, 2.4292(14) Å] in **2a** is normal.[44]

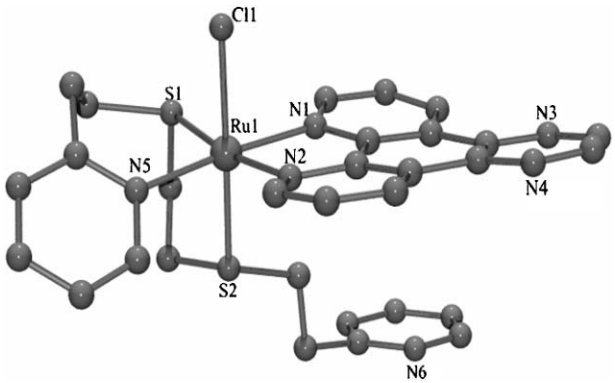


**Fig. 4** Ball-and-stick representation of the crystal structure of [Ru(pdto)(dpq)(Cl)]$^+$ cation **2a**; atoms as spheres of arbitrary diameter. Hydrogen atoms are omitted for clarity.

## $^1$H NMR spectra

The $^1$H NMR spectra of mononuclear Ru(II) complexes **1–6** show six aliphatic (**1–6**) and eight (**1**, **2**, **4**, **5**) or nine (**3**, **6**) aromatic signals indicating the presence of $C_2$ symmetry[45–47] in all the complexes. The protons in the coordinated pdto/bbdo are chemically equivalent while those of two halves of phen/dpq/dppz ligand are chemically as well as magnetically equivalent. The spectral patterns suggest a *trans* configuration for the two py (**1–3**)/bzim (**4–6**) rings and a *cis* configuration for the two py moieties of phen (**1**, **4**)/dpq (**2**, **5**)/dppz (**3**, **6**) ligands, as in the X-ray crystal structures of **1a**, **4a** and **5**. Also, the five- and six-membered chelate rings involving the –S–$CH_2$–$CH_2$–S– and –S–$CH_2$–$CH_2$–py/–S–$CH_2$–$CH_2$–bzim bridges exist in envelope and boat conformations respectively as in the X-ray crystal structures.

For all the Ru(II) complexes two different types of aromatic environments are observed due to two equivalent py (**1–3**; $H_a$–$H_d$) or bzim (**4–6**; $H_a$–$H_d$) rings in the axial positions and two equivalent py moieties of phen or dpq or dppz (**1–6**; $H_2$–$H_4$) ligands in the equatorial plane. In the case of **1** and **4** as well as **2** and **5** a third group of one individual resonance is observed for the benzene ring ($H_5$) of phen and quinoxaline ring ($H_7$) of dpq respectively. However, in **3** and **6** two individual resonances are observed for the phenazine ring ($H_8$ and $H_9$) of dppz. A positive shift is expected for both $H_c$ (**2**, **5**) and $H_d$ (**5**) protons but only negative shifts are observed. The upfield shifts observed for these protons are interesting and anomalous, as similar shifts have not been observed previously[48,49] for the Ru(II) complexes of py and bzim ligands. As coordination forces the dpq to be coplanar, the py/bzim rings in pdto/bbdo are obliged to rotate away from the dpq ring in order to minimize the steric interactions with it and renders these protons to be exposed to the shielding magnetic anisotropy of the ring current of dpq (*cf.* crystal structure of **5**). This reveals an unusual mode of coordination of aromatic ring nitrogens of pdto/bbdo ligand wherein steric interactions are relieved by lengthening the Ru–$N_{py}$/Ru–$N_{bzim}$ bond followed by rotation of the py/bzim rings about the bond between the aromatic ring and the adjacent aliphatic carbon atom. The positive c.i.s. (coordination-induced shift) values observed for $H_d$ (**1**, **2**, **3**, **6**) proton arise from a σ-effect based on electron donation to Ru(II) *via* the nitrogen lone pairs. Further, the positive c.i.s. values for $H_2$ (**1–6**), $H_3$ (**1**, **3–6**), $H_5$ (**1**, **4**) and $H_8$ and $H_9$ (**3**) protons of phen/dpq/dppz suggest that the ligand-to-metal σ-donation is more important (as this will decrease the electron density at these sites leading to positive c.i.s. values) than metal-to-ligand π-back donation in the ground state of these complexes. The conjugated system in the phen/dpq/dppz co-ligand may lead to a stronger ring current and electron-deficient characteristics and therefore cause the downfield chemical shifts of these protons. Analysis of the $^1$H NMR spectra of the dpq complexes **2** and **5** indicate that almost all the aromatic protons of **2** and **5** exhibit negative c.i.s. values, which are remarkably different from the aromatic protons of **1**, **3**, **4** and **6**. The upfield shifts of these aromatic protons are thought to result from interaction of the complex molecule with a neighbouring complex molecule in solution as found for other aromatic systems.[50]

## Electronic spectral and redox properties

In acetonitrile solution the complexes **1** and **4** with a phen co-ligand display two well-defined bands (**1**, 435, 400; **4**, 455, 415 nm) while **2** and **5** with dpq co-ligand and **3** and **6** with dppz co-ligand exhibit only a single absorption band in the range 430–465 nm. These bands arise from the dπ($Ru^{II}$) → π*(phen/dpq/dppz) metal-to-ligand charge-transfer (MLCT) transitions.[51–53] The absorptivity of the bands are higher for pdto (ε: **1**, 5050; **2**, 6197 and **3**, 7320 $M^{-1}$ $cm^{-1}$) than for bbdo complexes (ε: **4**, 3150; **5**, 3078 and **6**, 3140 $M^{-1}$ $cm^{-1}$) suggesting a higher distortion in the $RuN_4S_2$ chromophore of the former. Among the pdto (**1–3**) or bbdo (**4–6**) complexes substitution of a diimine ligand by another one with enhanced π-delocalization leads to lowering in energy of the dπ($Ru^{II}$) → π* MLCT band, as expected. Also, the

negative charge built on the metal by the strongly σ-donating bzim moieties in the bbdo complexes would be expected to destabilize the metal dπ orbital, thus lowering the $d\pi(Ru^{II}) \rightarrow \pi^*$ MLCT band energy (20–25 nm) relative to the pdto complexes. A similar lowering in band energy has been observed[54] for the MLCT band in $[Ru(bipy)_2(bibzim)]^{2+}$ and other $[Ru(bbdo)(L–L)]^{2+}$ complexes with symmetrical bidentate diimine (L–L) ligands. The higher energy bands observed in the range 250–375 nm arise from intraligand π–π* type transitions[55] involving energy levels higher in energy than the ligand LUMO levels. The complexes **1–6** exhibit no detectable luminescence in acetonitrile at room temperature. However, interestingly, the bzim complexes **4–6** exhibit a significant luminescence around 450 nm upon excitation at 295 nm while **1–3** fail to exhibit a similar luminescence in 100 mM $Na_2HPO_4/NaH_2PO_4$ and 0.5% of NaCl suggesting that the bzim moiety is involved in the emission.

In acetonitrile solution all the complexes exhibit a quasi-reversible ($\Delta E_p$, 76–96 mV; $i_{pc}/i_{pa}$, 0.7–1.1) metal-based oxidative response (Fig. 5, Table 3) with $E_{1/2}$ values falling in the range of 0.835–1.197 V. The high Ru(II)/Ru(III) redox potentials of the present chelates may be attributed to the π-acceptor ability of

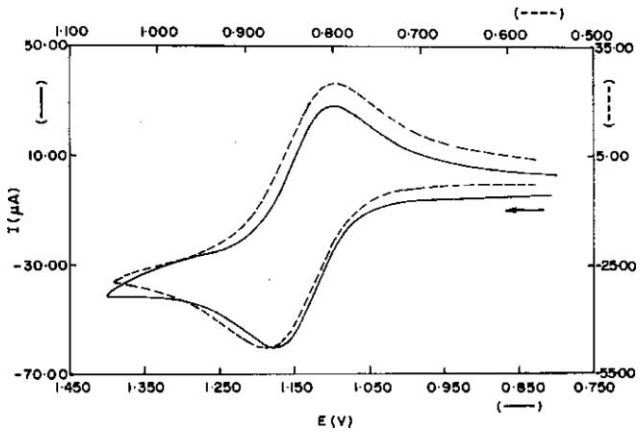


**Fig. 5** Cyclic voltammograms of 0.001 M complexes [Ru(pdto)(phen)]$(ClO_4)_2$ **1** (—) and [Ru(bbdo)(phen)]$(ClO_4)_2$ **4** (---) in $CH_3CN$ at 25 °C at 0.05 V $s^{-1}$ scan rate.

thioether donors in stabilizing the lower Ru(II) oxidation state. The Ru(II)/Ru(III) redox potentials of the bbdo complexes (**4–6**) are more negative than those for the corresponding pdto complexes (**1–3**), which is expected of the stronger σ-bonding of bzim moieties (*cf.* above) stabilizing the higher Ru(III) oxidation state. This trend is consistent with the lower MLCT band energies of the bbdo complexes (*cf.* above). For the bbdo complexes **4–6**, the Ru(II)/Ru(III) potentials become more positive as the diimine ligand is replaced by one with enhanced π-delocalization revealing the stabilization of the lower Ru(II) oxidation state, which is consistent with the decrease in MLCT band energy. However, among the pdto complexes (**1–3**) the dpq complex **2** possesses a Ru(II)/Ru(III) potential more positive than dppz complex **3**, which is inconsistent with the trend in the MLCT band energy. In this regard, it is to be noted that the $^1H$ NMR spectra for **2** and **5** are anomalous which is attributed to the presence of certain specific molecular interactions between primary and co-ligands. All the complexes display one or two irreversible reduction waves in the potential range −1.028 – −1.862 V, which arise from the addition of electrons in the electrochemically accessible LUMO[56] of the coordinated co-ligands rather than the pdto or bbdo ligand. In fact, free pdto or bbdo does not exhibit any ligand reduction in this range. Also, among the pdto (**1–3**) or bbdo (**4–6**) complexes the $E_{1/2}$ of ligand reduction becomes more positive as one moves from phen to dppz revealing facile addition of electrons to the more delocalized π* LUMO orbitals of the co-ligand.[57]

## DNA binding studies

### Absorption spectral studies

Upon the addition of calf thymus (CT) DNA to **1–6** ($R$ = [NP]/[Ru complex] = 0–40) in a 10% DMF–5 mM Tris-HCl–50 mM NaCl buffer at pH 7.1 at 25 °C interesting changes in intensity of the intense intraligand (IL) absorption bands of the complexes (264–364 nm) are observed—hypochromism for **2** and **3**, hypo- and then hyperchromism for **1** and **5**, hyperchromism for **4** and hyper- and then hypochromism for **6** (Fig. 6). The observed hypochromisms of 42 and 24% with red-shifts of 2 and 1 nm respectively for **2** and **3** (Fig. 7a, Table 4) unambiguously reveal the strong intercalation[58]

**Table 3** Redox properties of Ru(II) complexes[a,b,c] at 25.0 ± 0.2 °C

| Compound | $E_{pa}$/V | $E_{pc}$/V | $\Delta E_p$/mV | $E_{1/2}$[d]/V | $E_{1/2}$[e]/V | $i_{pc}/i_{pa}$ | $D \times 10^6$ $cm^2$ $s^{-1}$ |
|---|---|---|---|---|---|---|---|
| **1** | 1.172 | 1.098 | 74 | 1.137<br>−1.528<br>−1.786 | 1.135 | 0.9 | 11.0 |
| **2** | 1.238 | 1.156 | 82 | 1.197<br>−1.288<br>−1.654 | 1.195 | 1.1 | 6.7 |
| **3** | 1.210 | 1.130 | 80 | 1.142<br>−1.028 | 1.170 | 0.7 | 8.4 |
| **4** | 0.874 | 0.798 | 76 | 0.835<br>−1.862 | 0.836 | 0.9 | 4.7 |
| **5** | 0.958 | 0.862 | 96 | 0.910<br>−1.206 | 0.905 | 0.8 | 7.0 |
| **6** | 1.002 | 0.920 | 82 | 0.965<br>−1.104 | 0.961 | 0.8 | 9.2 |

[a] Measured *vs.* non-aqueous $Ag/Ag^+$ reference electrode; add 544 mV [300 mV, $Ag/Ag^+$ to SCE + 244 mV, SCE to SHE] to convert to standard hydrogen electrode (SHE); scan rate, 50 mV $s^{-1}$; supporting electrolyte, $[(C_4H_9)_4N](ClO_4)$ (0.1 M). [b] Complexes **1–6** in acetonitrile. [c] Negative values are ligand reduction potential. [d] Redox potentials correspond to $Ru^{II}/Ru^{III}$ couple. [e] Differential pulse voltammetry, scan rate, 1 mV $s^{-1}$; pulse height, 50 mV.

 

**Table 4** Absorption spectral properties of Ru(II) complexes bound[a] to CT DNA

| Complex | $\lambda_{max}$/nm | $R$ | Change in absorbance | $\Delta\varepsilon$(%) | Redshift/nm | $K_b \times 10^{-6}$/M | $s^b$ |
|---|---|---|---|---|---|---|---|
| $[Ru(pdto)(phen)]^{2+}$ **1** | 264 | 40 | Hyper- and hypochromism | — | — | —[c] | — |
| $[Ru(pdto)(dpq)]^{2+}$ **2** | 269 | 40 | Hypochromism | 42 | 2 | 0.020 ± 0.002 | 1.0 |
| $[Ru(pdto)(dppz)]^{2+}$ **3** | 357 | 40 | Hypochromism | 27 | 1 | 3.00 ± 0.01 | 1.3 |
| $[Ru(bbdo)(phen)]^{2+}$ **4** | 269 | 40 | Hyper- and hypochromism | — | — | —[c] | — |
| $[Ru(bbdo)(dpq)]^{2+}$ **5** | 256 | 40 | Hyper- and hypochromism | — | — | —[c] | — |
| $[Ru(bbdo)(dppz)]^{2+}$ **6** | 364 | 40 | Hyper- and hypochromism | — | — | —[c] | — |

[a] Measurement were made at $R = 40$, where $R$ = [DNA]/[Ru complex], concentration of ruthenium(II) complex solutions = $7.6 \times 10^{-5}$ M (**1**), $5 \times 10^{-5}$ M (**2** and **3**), $2 \times 10^{-5}$ M (**4**), and $8.5 \times 10^{-5}$ M (**5** and **6**); [b] Binding site size in base pairs; [c] Binding constants not calculated as spectral changes are not uniform.

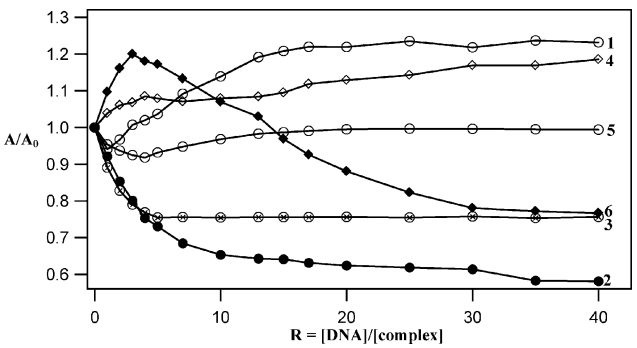


**Fig. 6** Effect of addition of DNA on the absorption intensity of the complexes **1**, 264; **2**, 269; **3**, 357; **4**, 269; **5**, 256; **6**, 364 nm in a 10% DMF–5 mM Tris-HCl–50 mM NaCl buffer at pH 7.1 and 25 °C.

of coordinated dpq and dppz ligands in between the DNA base pairs. The mixed behavior for other complexes reveals more than one DNA binding mode. From the observed spectral changes for **2** and **3** the values of the intrinsic equilibrium DNA binding constant $K_b$ was determined by regression analysis using eqn (1) (Fig. 7b),[59] which includes binding site size.

$$(\varepsilon_a - \varepsilon_f)/(\varepsilon_b - \varepsilon_f) = (b - (b^2 - 2K_b{}^2C_t[DNA]_t/s)^{1/2})/2K_bC_t \quad (1a)$$

$$b = 1 + K_bC_t + K_b[DNA]_t/2s \quad (1b)$$

where $\varepsilon_a$ is the extinction coefficient observed for the absorption band at a given DNA concentration, $\varepsilon_f$ is the extinction coefficient of the complex free in solution, $\varepsilon_b$ is the extinction coefficient of the complex when fully bound to DNA, $K_b$ is the equilibrium binding constant, $C_t$ is the total metal complex concentration, [DNA] is the DNA concentration in nucleotides, and $s$ is the binding site size in base pairs. The $K_b$ value obtained for complex **3** ($3.0 \times 10^6$ $M^{-1}$) is higher than **2** ($2.0 \times 10^4$ $M^{-1}$), which is expected of the deeper intercalation of the dppz ligand with a larger surface area (Table 4). It is of the same order as that reported for $[Ru(phen)_2(dppz)]^{2+}$ ($5.1 \times 10^6$ $M^{-1}$),[60] which has been shown to bind to DNA through intercalation of the dppz ligand. But it is lower than that for $[Ru(ip)_2(dppz)]^{2+}$ ($2.1 \times 10^7$ $M^{-1}$),[61] which is expected as the ethylene moieties in **3** could prevent the complex from efficient DNA binding. Thus the value of $K_b$ is higher than that reported for $[Ru(NH_3)_4(dppz)]^{2+}$ ($1.24 \times 10^5$ $M^{-1}$), suggesting that the intercalative binding of the dppz ligand in **3** is stronger than that in the latter.[60] The binding site size (1.3) of **3** is higher than those reported for $[Ru(phen)_2(dppz)]^{2+}$ (0.6),[60] $[Ru(ip)_2(dppz)]^{2+}$ (0.4),[61] and $[Ru(NH_3)_4(dppz)]^{2+}$ (0.02),[60] which is consistent with

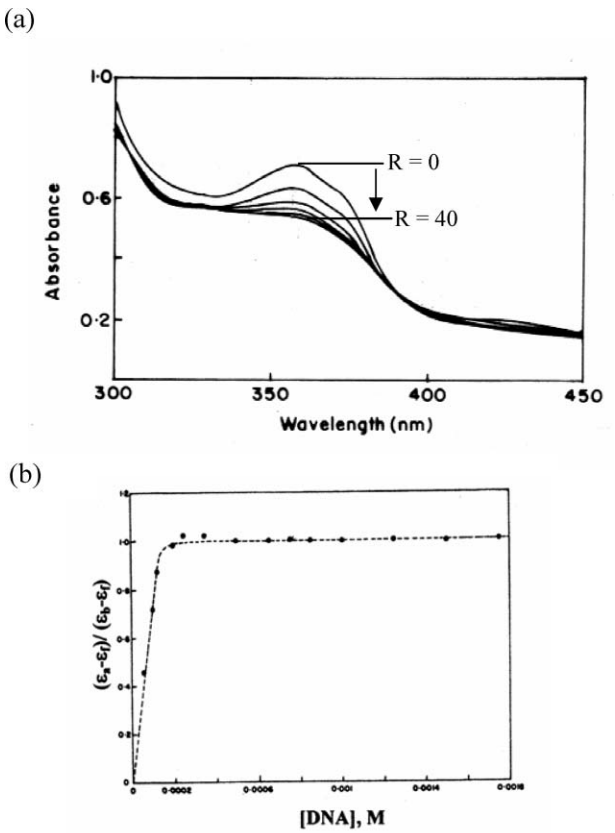


**Fig. 7** (a) Absorption spectra of $[Ru(pdto)(dppz)]^{2+}$ ($5 \times 10^{-5}$ M) in a 10% DMF–5 mM Tris-HCl–50 mM NaCl buffer at pH 7.1 ($R$ = [DNA]/[complex] = 0) and presence ($R$ = 1–40) of increasing amounts of DNA. (b) The plot of $(\varepsilon_a - \varepsilon_b)/(\varepsilon_b - \varepsilon_f)$ *vs.* [DNA] for $[Ru(pdto)(dppz)]^{2+}$. The best fit line, superimposed on the data, according to eqn (1a), (1b) yields $K_b = 3.0 \times 10^6$ $M^{-1}$ and $s = 1.3$.

the involvement of more DNA base pairs in interaction with the sterically bulky complex **3**.

In contrast to **2** and **3**, the phen complex **1** exhibits a hyperchromism, which remains constant beyond $R = 20$. Electrostatically bound on the surface of DNA it appears to undergo distortion in the coordination sphere resulting in the enhanced allowedness of the intraligand band. A similar but lower hyperchromism observed for the analogous phen complex **4** is expected of its less intimate DNA binding because of the bulky bzim moieties of the bbdo ligand. Interestingly, the complex **6**, in spite of it containing dppz ligand with extended aromatic ring, also

shows a higher hyperchromism at lower DNA concentrations but hypochromism at higher concentrations of DNA as for the analogous pdto complex **3**. It is likely that the hyperchromism arises from aggregation of the complex molecules *via* π–π stacking of dppz ligands on the DNA surface and/or from the intimate surface binding of **6** with the two bzim rings stacked along the DNA backbone.[62] The complex **5** shows a hypochromism lower than its pdto analogue **2** even at higher DNA concentrations because of less intimate partial intercalation of the dpq ligand dictated by bulky bzim moiety of bbdo.

### Competitive DNA binding studies

On adding the complexes **1–6** (0–60 μM) to DNA pretreated with ethidium bromide ($R$ = [DNA]/[EthBr] = 10) the emission intensity of DNA-bound EthBr ($\lambda_{ex}$, 450; $\lambda_{em}$, 595 nm) decreases (Fig. 8). From the plot of these intensities against complex concentration the values of the apparent DNA binding constant ($K_{app}$) were calculated[63] using the equation

$$K_{EthBr}[EthBr] = K_{app}[Complex]$$

where $K_{EthBr}$ is $1.0 \times 10^7$ $M^{-1}$, the concentration of EthBr is 12.5 μM and the concentration of the complex is that used to obtain a 50% reduction in fluorescence intensity of EthBr. The DNA binding abilities of the complexes follow the order: **6** > **3** > **5** > **2** > **4** > **1** (Fig. 8). The dicationic complexes **6** and **3** involved in strong DNA intercalation are expected to compete more strongly with the intercalatively bound monopositive ethidium cation than other complexes. We propose that hydrogen bonding interactions occur between the bzim-NH of bbdo in **6** and functional groups present on the edge of the DNA,[13b] and incorporation of the more hydrophobic[9c] bzim moiety would contribute significantly to the higher DNA binding affinity of **6**. Thus H-bonding[64] and ligand hydrophobicity as in Ru(II) arene complexes,[9c] in addition to direct coordination to the bases and intercalation, are useful features for incorporation into the design of Ru(II) complexes to optimize their recognition of DNA. Further, on the addition of **1–6** ($R$ = 1 = [dye]/[complex]) to DNA pretreated with the dye Hoechst 33258 ($R$ = 10 = [DNA]/[complex]), an appreciable reduction in emission intensity of the DNA-bound dye ($\lambda_{ex}$, 450; $\lambda_{em}$, 595 nm, Fig. 9)[65] is observed. As the present complexes do not have any effect on the emission of Hoechst 33258 in the absence

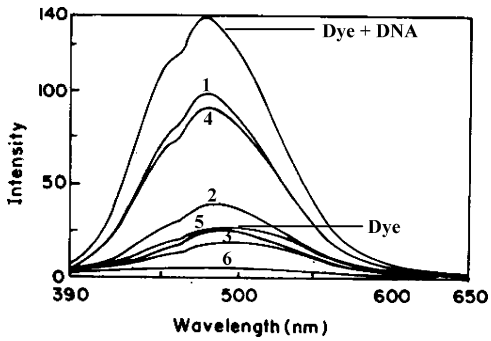


**Fig. 9** Effect of addition of **1–6** on the emission intensity of the CT DNA-bound Hoechst 33258 (125 μM) in a 10% DMF–5 mM Tris-HCl–50 mM NaCl buffer at pH 7.1 and 25 °C.

of DNA, any termolecular binding, which is expected to cause the quenching of emission of the minor groove bound dye,[66] is either impossible or extremely unlikely.[67] So, it appears that the present Ru(II) complexes compete with Hoechst 33258 to bind strongly in the DNA minor groove.

### Thermal denaturation and viscosity measurements

The complexes **1–6** were incubated with CT DNA at $1/R = 0.1$, the solution temperature raised from 25 to 95 °C and the absorbance at 260 nm was monitored. The observed $\Delta T_m$ ($T_m$ of CT DNA bound to complex-$T_m$ of CT DNA) values vary in the order **6** (10 ± 1) > **3** (7 ± 1) > **5** (4 ± 1) > **2** (3 ± 1) > **4** (2.7 ± 1.0) > **1** (2.3 ± 1.0 °C). The $\Delta T_m$ values of **6** and **3** fall in the range for classical intercalators[68] suggesting that intercalation of the planar aromatic moiety of dppz in between the DNA base pairs more strongly than the dpq co-ligand leads to a higher melting temperature of the double-stranded DNA bound to **6**. When **1–6** are treated with CT DNA (200 μM) and the concentration of ruthenium complex is increased from $1/R$ = 0–0.5 ($1/R$ = [Ru]/[DNA]), the relative viscosity of DNA increases (Fig. 10) in the order **6** > **3** > **5** > **2** > **4** > **1**. This supports the results from competitive DNA binding studies and thermal denaturation studies. The highest increase in DNA viscosity effected by **6** and **3** is similar to that observed for proven intercalators[69] suggesting that the complexes dramatically

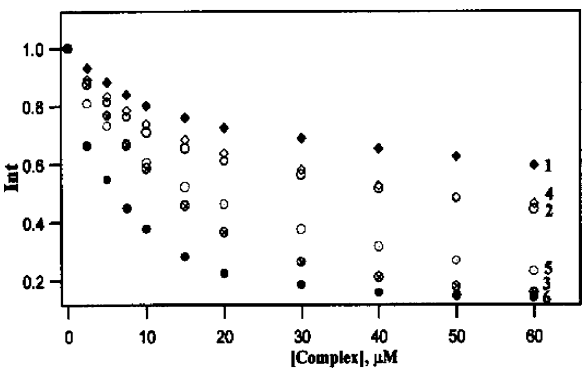


**Fig. 8** Effect of addition of **1–6** on the emission intensity of the CT DNA-bound ethidium bromide (125 μM) at different complex concentrations in a 10% DMF–5 mM Tris-HCl–50 mM NaCl buffer at pH 7.1 and 25 °C.

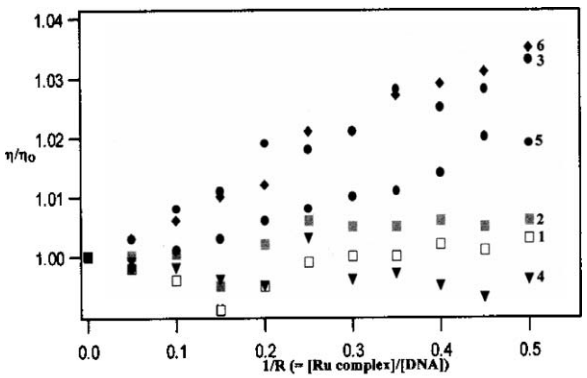


**Fig. 10** The effect of addition of **1–6** on the viscosity of CT DNA in a 10% DMF–5 mM Tris-HCl–50 mM NaCl buffer at pH 7.1; Relative specific viscosity *vs.* $1/R$; [CT DNA] = 200 μM.

 

increase the hydrodynamic length of DNA as a consequence of the untwisting of the base pairs and helical backbone of DNA needed to accommodate the intercalators.[13b]

### Electrochemical studies

The cyclic (CV) and differential pulse voltammetric (DPV) responses have been obtained for **1–6** on an ITO electrode in 10% DMF–5 mM Tris-HCl–50 mM NaCl buffer at pH 7.1 in the presence and absence of DNA and the well-behaved DPV responses are used to monitor the interaction of the complexes with DNA (Table 5). The redox potentials of the Ru(II)/Ru(III) couple ($E^{0\prime}$ or voltametric $E_{1/2}$) for the pdto complexes (**1**, 1.287; **2**, 1.415; **3**, 1.345 V) are higher than those for their bbdo analogues (**4**, 0.831; **5**, 0.847; **6**, 0.803 V), which is consistent with the general trends in $E_{1/2}$ values in acetonitrile solution (*cf.* above). On the incremental addition of CT DNA to the metal complexes ($R$ = 0.25–3), a drop in the peak currents of the anodic waves in the CV and of DPV response for **1**, **2**, **5** and **6** (Fig. 11a) is observed, and the value of $i_{pa}$ decreases regularly with increase in DNA concentration. This indicates the slower mass transfer of the complexes bound to DNA fragments,[70] which leads to a decrease in concentration of the unbound redox-active species in solution. In contrast, the anodic peak currents of **3** (Fig. 11b) and **4** are higher than those in the absence of DNA indicating that multiple turnovers of oxidation of DNA by the oxidized Ru(III) form of the metal complexes occur during a single voltammetric sweep.[71] Similar catalytic enhancement of anodic current has been observed on ITO electrode when complexes like $[Ru(diimine)_3]^{2+}$, where diimine = bpy, phen and 5,6-dmp,[18b,72] are interacted with CT DNA. It is obvious that the strongly DNA-bound **1**, **2**, **5** and **6** Ru(III) species are immobilized on DNA rendering them incapable of moving to other parts of the biopolymer and effect the oxidation of guanine in DNA. Further, the shift in $E_{1/2}$ of **3–6** to a more positive potential (17–100 mV) on binding to DNA reveals that the oxidation of Ru(II) to Ru(III) is rendered difficult. On the other hand, the $E_{1/2}$ of **1** and **2** become less positive (13, 17 mV) on binding to DNA revealing that the oxidation of Ru(II) to Ru(III) becomes facile. Thus the DNA surface-bound complex **4** exhibits guanine oxidation and in fact it has been previously reported that DNA surface-bound complexes like $[Ru(diimine)_3]^{2+}$ exhibit electrocatalytic oxidation of guanine.[18b,72]

**Table 5** Cyclic and differential pulse voltammetric behaviour[a] of Ru(II) complexes in the absence and presence of CT DNA ($R$ = [DNA]/[Ru]) at 25.0 ± 0.2 °C

| | | | | $E_{1/2}$/V | | |
|---|---|---|---|---|---|---|
| Compound | $R$ | $E_{pa}$/V | $E_{pc}$/V | CV | DPV | $\Delta E_p$/mV |
| $[Ru(pdto)(phen)]^{2+}$ **1** | 0.0 | 1.312 | 1.248 | 1.280 | 1.287 | 64 |
| | 3.0 | 1.324 | 1.234 | 1.297 | 1.690 | 90 |
| $[Ru(pdto)(dpq)]^{2+}$ **2** | 0.0 | 1.468 | 1.326 | 1.397 | 1.415 | 142 |
| | 3.0 | 1.498 | 1.366 | 1.432 | 1.403 | 132 |
| $[Ru(pdto)(dppz)]^{2+}$ **3** | 0.0 | 1.448 | 1.282 | 1.365 | 1.345 | 166 |
| | 2.0 | 1.456 | 1.292 | 1.374 | 1.363 | 164 |
| $[Ru(bbdo)(phen)]^{2+}$ **4** | 0.0 | 0.888 | 0.756 | 0.822 | 0.831 | 132 |
| | 3.0 | 0.958 | 0.774 | 0.869 | 0.919 | 178 |
| $[Ru(bbdo)(dpq)]^{2+}$ **5** | 0.0 | 0.930 | 0.784 | 0.857 | 0.847 | 146 |
| | 0.5 | 0.904 | 0.780 | 0.842 | 0.853 | 124 |
| $[Ru(bbdo)(dppz)]^{2+}$ **6** | 0.0 | 0.888 | 0.740 | 0.814 | 0.803 | 148 |
| | 0.5 | 0.878 | 0.736 | 0.807 | 0.827 | 142 |

[a] Measured *vs.* saturated calomel electrode; add 0.244 to convert to normal hydrogen electrode (NHE); Scan rate 50 mV $s^{-1}$; supporting electrolyte 50 mM NaCl; complex concentration 0.25 × $10^{-3}$; Differential pulse voltammetry (DPV), scan rate 2 $mVs^{-1}$; pulse height 50 mV; working electrode ITO.

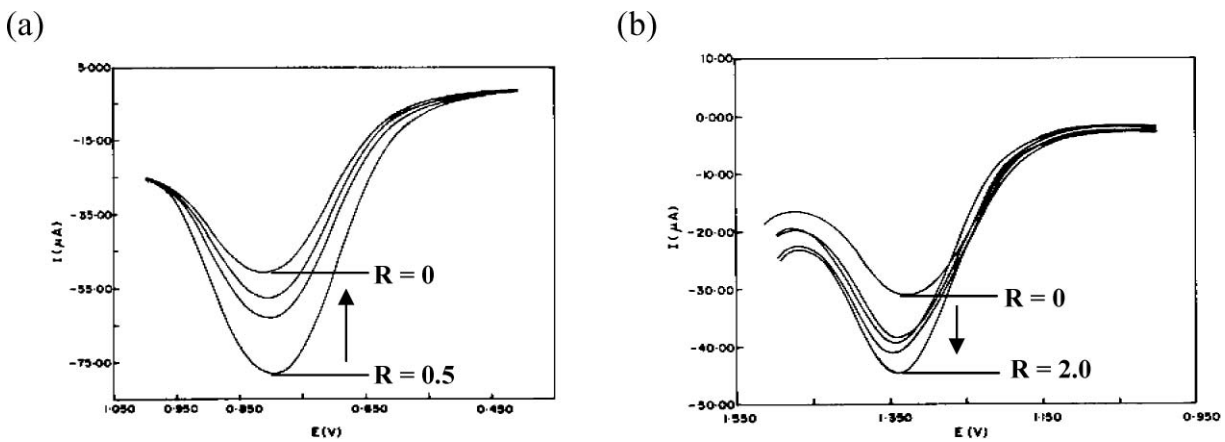


**Fig. 11** (a) Differential pulse voltammograms of 0.25 mM $[Ru(bbdo)(dppz)]^{2+}$ **6** in the absence ($R$ = 0) and presence ($R$ = 0.25–0.5) of CT DNA (b) Differential pulse voltammograms of 0.25 mM $[Ru(pdto)(dppz)]^{2+}$ **3** in the absence ($R$ = 0) and presence ($R$ = 0.25–2.0) of CT DNA. Scan rate 5 mV $s^{-1}$; pulse height 50 mV; supporting electrolyte, 50 mM NaCl; working electrode ITO.

However, involvement of the intercalatively DNA-bound **3** in electrocatalytic guanine oxidation is interesting and it is possible that the partial intercalation of the dppz complex enables its closer approach to guanine of DNA.

### Interaction with supercoiled pBR322 DNA

The interaction of complexes **1–6** with supercoiled pBR322 DNA in 10% DMF–5 mM Tris-HCl–50 mM NaCl buffer at pH 7.1 was studied by agarose gel electrophoresis. The complexes (60 μM) were incubated with DNA (40 μM base pairs) for 1 h and then subjected to gel electrophoresis. The electrophorogram shows (lanes 2–6, Fig. 12a) a pattern for **1–5**, which is very similar to the control indicating that the plasmid DNA is not cleaved. In contrast, lane 7 for **6** contains no band corresponding to SC (supercoiled) or any cleaved NC (nicked circular) (form II) or LC (linear circular) form (form III); however, a very faint band is discerned in the well. It is obvious that the complex **6**–DNA adduct is made discernible by the EthBr (used to stain DNA) bound to it. When the concentration of **6** is varied from 0 to 100 μM keeping the DNA concentration (40 μM) constant, interestingly, the free SC form is discernible at low concentrations of complex (20, 40 μM) as for the control and **1–5**, and a faint band corresponding to **6**–DNA–EthBr is discerned in the well (Fig. 12b). At a 60 μM concentration of complex no SC form is detected but, as expected, the faint band is still present in the well. At complex concentrations of 80 μM and above, no SC form or **6**–DNA–EthBr adduct in the well is discerned revealing that EthBr is completely expelled from the plasmid due to high concentration of complex leading to quenching of the EthBr emission (*cf.* above, competitive binding studies). When plasmid DNA concentration is varied from 0 to 150 μM by keeping the concentration of **6** constant at 60 μM, the **6**–DNA–EthBr adduct is not detected in the well at 20 μM DNA but both SC form and adduct are discernible beyond 80 μM DNA as unbound DNA is available at low concentrations of **6** (Fig. 12c). All the above observations suggest the formation of an approximately 1 : 1 : 1 DNA : **6**: EthBr adduct. Also, experiments were conducted by varying the incubation time from 0–60 min, keeping the concentrations of complex (60 μM) and DNA (40 μM) constant. After 5 min of incubation time, the adduct **6**–DNA–EthBr is discernible in the well but no SC form is visible. Also, for longer incubation times the adduct is discernible (Fig. 12d). The formation of the strong DNA–**6** adduct is unique and is not observed for the analogous complexes **1–5**.

In order to investigate the involvement of the reactive oxygen species (ROS) on DNA adduct formation of **6** the DNA was treated with various radical scavengers like DMSO (hydroxyl radical), $NaN_3$ (singlet oxygen) and SOD (superoxide dismutase) and catalase ($H_2O_2$) (Fig. 12e) for 5 min and then incubated with **6** (60 μM). It was found that all the scavengers, except DMSO and catalase, fail to inhibit the DNA adduct formation. It is possible that DMSO and catalase would inhibit **6**–DNA adduct formation. Also, under rigorously anaerobic (hypoxy) conditions the DNA adduct formation of **6** is not inhibited (Fig. 12e). Thus it is clear that freely diffusible radicals are not involved in the DNA adduct formation. We reason that the intercalator molecule dramatically untwists the plasmid DNA (*cf.* above) leading to bulging and condensation.[73] The structural changes and alteration in the superhelicity[74] of closed circular DNA lead to increased

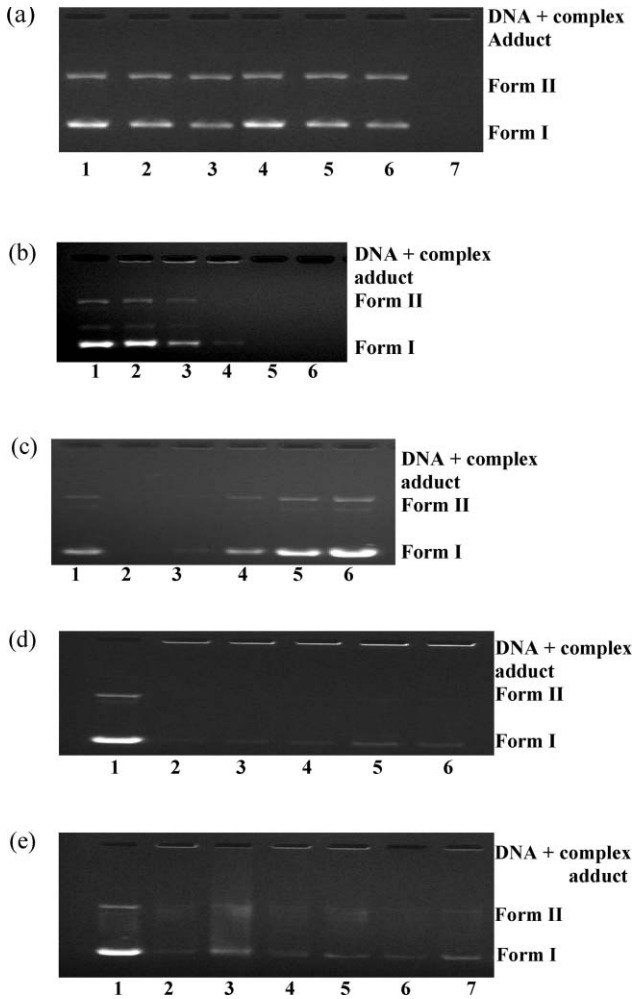


**Fig. 12** (a) Gel electrophoresis diagram showing the interaction of complexes **1–6** (60 μM) with supercoiled pBR322 DNA (40 μM in base pair) without added reductant and irradiation in a 10% DMF–5 mM Tris-HCl–50 mM NaCl buffer at pH 7.1 and 37 °C with an incubation time of 1 h. Lane 1, DNA; lane 2, DNA + **1**; lane 3, DNA + **2**; lane 4, DNA + **3**; lane 5, DNA + **4**; lane 6, DNA + **5**; lane 7, DNA + **6**. Forms I and II are supercoiled and nicked circular forms of DNA respectively. (b) Various concentrations of **6** were reacted with supercoiled pBR322 plasmid DNA (40 μM in base pair) with an incubation time of 10 min in a 10% DMF–5 mM Tris-HCl–50 mM NaCl buffer at pH 7.1. Lane 1, DNA control; lane 2, DNA + **6** (20 μM); lane 3, DNA + **6** (40 μM); lane 4, DNA + **6** (60 μM); lane 5, DNA + **6** (80 μM); lane 6, DNA + **6** (100 μM). (c) Various concentrations of supercoiled pBR322 plasmid DNA were reacted with a constant concentration of the complex **6** (60 μM) with an incubation of 10 min in a 10% DMF–5 mM Tris-HCl–50 mM NaCl buffer at pH 7.1 and 37 °C. Lane 1, supercoiled DNA 40 μM; lane 2, 40 μM DNA + **6**; lane 3, 60 μM DNA + **6**; lane 4, 80 μM DNA + **6**; lane 5, 120 μM DNA + **6**; lane 6, 150 μM DNA + **6**. (d) Time course of interaction of **6** (60 μM) with supercoiled pBR322 plasmid DNA (40 μM in base pair) in a 10% DMF–5 mM Tris-HCl–50 mM NaCl buffer at pH 7.1 and 37 °C with an incubation times of 0, 5, 10, 20, 30 and 60 min for lanes 2–6 (e) Interaction of **6** (60 μM) with supercoiled pBR322 plasmid DNA (40 μM in base pair) in the presence of various radical scavengers. Lane 1, DNA (40 μM in base pair); lane 2, DNA + **6** (60 μM); lane 3, DNA + **6** (60 μM) 10% DMSO; lane 4, DNA + **6** (60 μM) + 50 μM $NaN_3$; lane 5, DNA + **3** (60 μM) + SOD (1 unit); lane 6, DNA + **6** (60 μM) + catalase (0.1 unit); lane 7, DNA + **6** (60 μM) + argon atmosphere.

 

frictional force between DNA and the gel matrix, which retard[13b] the mobility of the adduct during electrophoresis and thus the band in the well corresponds to a DNA–intercalator–EthBr adduct at lower concentrations of **6** (40–60 μM). At higher concentrations of **6** (80–100 μM) the adduct could not be detected revealing that the DNA bound-intercalator might untwist the DNA duplex expelling the bound EthBr and quenching its emission intensity (*cf.* above).[13b] Similar inaccessibility of EthBr to plasmid DNA, which becomes compact on binding to polyethyleneimines, has been observed previously.[75] The ability of **1–6** (60 μM) to effect photo-induced DNA strand scission was also examined by incubating them with supercoiled pBR322 DNA (40 μM base pairs) in a 10% DMF–5 mM Tris-HCl–50 mM NaCl buffer at pH 7.1 for 1 h. After irradiation with monochromatic radiation of 365 nm it is found that all the complexes fail to cleave the DNA.

### Cytotoxicity of Ru(II) complexes

The two complexes **3** and **6**, which show strong DNA binding, have been screened against all cell lines of different cancer origins, *viz.* melanoma (A375), breast cancer (MDAMB-435 and MDAMB-468), glioblastoma (U373), fibrosarcoma (HT1080) and lung carcinoma (H460). Both the compounds are also checked for their toxic effects on HaCaT cells, which are human immortalized keratinocytes used as representatives of normal cells. For comparison, the cytotoxicities of the two known anticancer drugs, *viz.* adriamycin and cisplatin have also been assessed against all the above cell lines. The above DNA binding studies reveal that the dppz complex **6** exhibits stronger DNA binding than **3** and that only **6** forms a well-condensed adduct with supercoiled pBR322 DNA. As **6** alone exhibits a cytotoxicity (Table 6) higher than **3**, it is evident that besides the dppz co-ligand, the hydrophobic bzim moiety in the bbdo ligand plays an important role in conferring the interesting biological activity on **6**, like Ru(II) arene complexes.[9c] Also, **6** exhibits significant cytotoxicity against all the cell lines, except MDAMB-435. Remarkably, it exhibits the highest activity against melanoma cells (A375) with an $IC_{50}$ value of 4.0 μM (Table 6) and also exhibits a potency approximately 2 times more than cisplatin ($IC_{50}$, 7.7 μM) against A375 but 40 times less than adriamycin. The cytotoxicity results also indicate that the toxicity of **6** towards HaCaT cells is about 90 times less than that of adriamycin and about 3 times less than that of cisplatin. The $IC_{50}$ value of **6** against HaCaT cells (4.2 μM) is also slightly higher than that of A375 (4.0 μM) while this is not the case with adriamycin and cisplatin. The $IC_{50}$ value of the latter two drugs in A375 cells is higher than that in the HaCaT cells, which means that their cytotoxic levels in cancer cells are above their toxic levels in normal cells. In other words, compared to adriamycin and cisplatin, the activity of **6** in melanoma cells is at a concentration that is slightly less toxic to normal cells. This is interesting as melanoma, which is the most aggressive form of skin cancer, is resistant to most chemotherapeutic drugs.[76–78] Dacarbazine or DTIC, which is the chemotherapeutic drug used for advanced melanoma, is the only one approved by the FDA for this purpose. But the overall response rate ranges from 10 to 20% with complete remissions only in 5% of the cases.[77] Other drugs like cisplatin, carboplatin, taxol and vinblastine have not been found to be better than DTIC.[77] Studies *in vivo* have shown that melanoma cells are resistant to DTIC, cisplatin and other chemotherapeutic drugs.[79] Also, none of the currently known therapies for melanoma seem to prolong survival.[80] In this scenario, the discovery of **6** as a new promising chemotherapeutic and less toxic drug against melanoma assumes significance.

**Table 6** *In vitro* cytotoxicity assays for complexes $[Ru(pdto)(dppz)]^{2+}$ **3**, $[Ru(bbdo)(dppz)]^{2+}$ **6**, adriamycin and cisplatin screened against cell lines of different cancer origins, *viz.* melanoma (A375), breast cancer (MDAMB-435 and MDAMB-468), glioblastoma (U373), fibrosarcoma (HT1080) and lung carcinoma (H460). Standard deviations are given immediately after $IC_{50}$ values

| | Drug [a] ($IC_{50}$/μM by MTT assay) | | | |
|---|---|---|---|---|
| Cell lines | **3** | **6** | Adriamycin | Cisplatin |
| A375 | >113 | 4.0 ± 0.7 | 0.01 ± 0.02 | 7.7 ± 0.1 |
| MDAMB-435 | >113 | >104 | >2 | >23.0 |
| MDAMB-468 | 54.0 ± 0.8 | 20.00 ± 0.03 | 0.50 ± 0.06 | 8.0 ± 0.1 |
| U373 | >113 | 7.3 ± 0.2 | 0.07 ± 0.01 | 5.0 ± 0.9 |
| HT1080 | >113 | 28.00 ± 1.40 | 0.080 ± 0.004 | 8.0 ± 0.09 |
| H460 | 21.0 ± 1.4 | 12.0 ± 0.7 | 0.10 ± 0.03 | 1.4 ± 0.2 |
| HaCaT | 8 ± 0.02 | 4.2 ± 0.09 | 0.050 ± 0.005 | 1.6 ± 0.06 |

[a] $IC_{50}$ = concentration of drug required to inhibit growth of 50% of the cancer cells.

## Conclusions

In the mixed ligand Ru(II) complexes $[Ru(pdto/bbdo)(diimine)]^{2+}$ the coordinated diimine co-ligands phen, dpq and dppz are involved in partial intercalation into the DNA base pairs in the minor groove region, with the dppz complexes displaying stronger DNA binding affinity. Interestingly, the complexes $[Ru(bbdo)(phen)]^{2+}$ and $[Ru(pdto)(dppz)]^{2+}$ effect electrochemical oxidation of the guanine moiety of DNA. It is remarkable that, of all the complexes, $[Ru(bbdo)(dppz)]^{2+}$ alone alters the superhelicity of supercoiled pBR322 DNA in the absence of any external reagent or light and forms the strongest complex–DNA–EthBr adduct. Also, it is noteworthy that the same complex exhibits higher anticancer activity than its pdto analogue, more potency than cisplatin against the melanoma (A375) cell line and also 3 and 90 times less toxicity towards normal cells than cisplatin and adriamycin respectively. So it is disclosed that the coordinated bzim moieties with H-bonding motifs and capable of being involved in hydrophobic interactions and the affinity ligand dppz have significant potentials as substructures for designing newer metal-based anticancer drugs. To the best of our knowledge this complex is the first non-covalently DNA binding mixed ligand Ru(II) complex exhibiting cytotoxicity against melanoma. Studies are in progress to elucidate the extraordinary behavior of the complex in more detail by unraveling the detailed molecular mechanism of its cytotoxicity.

## Acknowledgements

Council of Scientific and Industrial Research, New Delhi, India is thanked for financial support (Grant No. 01(2101)/07/EMR-II) and for SRF to V. R. Professor M. Palaniandavar is Ramanna Fellow of Department of Science and Technology, New Delhi, India. We thank Professor K. Natarajan, Department of

Chemistry, Bharathiyar University, Coimbatore, for obtaining the CHN data. We thank Dr Babu Varghese and Dr Moni, Regional Sophisticated Instrumentation Centre, Indian Institute of Technology, Chennai, for obtaining some of the X-ray data and recording NMR respectively. University Grants Commission (UGC), New Delhi and Department of Science and Technology, New Delhi are greatly acknowledged for funding to generate an Instruments Facility in the Department through the Special Assistance Program (SAP) of UGC and the Funds for Improvement of S&T Infrastructure (DST-FIST) Program of the Department of Science and Technology, New Delhi respectively.

## References


1 B. Rosenberg, L. Van Camp, J. E. Trosko and V. H. Mansour, *Nature*, 1969, **222**, 385.
2 (*a*) E. R. Jamieson and S. J. Lippard, *Chem. Rev.*, 1999, **99**, 2467; (*b*) E. Wong and C. M. Giandomenico, *Chem. Rev.*, 1999, **99**, 2451.
3 (*a*) A. C. G. Hotze, S. E. Caspers, D. de Vos, H. Kooijman, A. L. Spek, A. Flamigni, M. Bacac, G. Sava, J. G. Haasnoot and J. Reedijk, *JBIC, J. Biol. Inorg. Chem.*, 2004, **9**, 354; (*b*) A. C. G. Hotze, B. M. Kariuki and M. J. Hannon, *Angew. Chem., Int. Ed.*, 2006, **45**, 4839.
4 (*a*) C. G. Hartinger, S. Zorbas-Seifried, M. A. Jakupec, B. Kynast, H. Zorbas and B. K. Keppler, *J. Inorg. Biochem.*, 2006, **100**, 891; (*b*) M. Galanski, V. B. Arion, M. A. Jakupee and B. K. Keppler, *Curr. Pharm. Des.*, 2003, **9**, 2078.
5 (*a*) M. A. Fuertes, C. Alonso and J. Perez, M., *Chem. Rev.*, 2003, **103**, 645; (*b*) M. J. Clarke, F. C. Zhu and D. R. Frasca, *Chem. Rev.*, 1999, **99**, 2511.
6 (*a*) M. Cocchietto and G. Sava, *Pharmacol. Toxicol.*, 2000, **87**, 193; (*b*) S. Zorzet, A. Sorc, C. Casarsa, M. Cocchietto and G. Sava, *Met-Based Drugs*, 2001, **8**, 1; (*c*) R. Gagliardi, G. Sava, S. Pacor, G. Mestroni and E. Alessio, *Clin. Exp. Metastasis*, 1994, **12**, 93; (*d*) M. Magnarin, A. Bergamo, M. E. Carotenuto, S. Zorzet and G. Sava, *Anticancer Res.*, 2000, **20**, 2939; (*e*) J. M. Rademaker-Lakhai, D. Van den Bongard, D. Pluim, J. H. Beijnen and J. H. Schellens, *Clin. Cancer Res.*, 2004, **10**, 3717.
7 (*a*) G. Sava, K. Clerici, I. Capozzi, M. Cocchietto, R. Gagliardi, E. Alessio and G. Mestroni, *Anti-Cancer Drugs*, 1999, **10**, 129; (*b*) G. Sava, R. Gagliardi, A. Bergamo, E. Alessio and G. Mestroni, *Anticancer Res.*, 1999, **19**, 969; (*c*) G. Sava, R. Gagliardi, M. Cocchietto, K. Clerici, I. Capozzi, M. Marella, E. Alessio, G. Mestroni and R. Milanino, *Pathol. Oncol. Res.*, 1998, **4**, 30.
8 (*a*) B. K. Keppler, M. Henn, U. M. Juhl, M. R. Berger, R. Niebl and F. E. Wagner, *Prog. Clin. Biochem. Med.*, 1989, **10**, 41; (*b*) E. D. Kreuser, B. K. Keppler, W. E. Berdel, A. Piest and E. Thiel, *Semin. Oncol.*, 1992, **19**, 73.
9 (*a*) R. E. Morris, R. E. Aird, P. D. Murdoch, H. M. Chen, J. Cummings, N. D. Hughes, S. Parsons, A. Parkin, G. Boyd, D. I. Jodrell and P. J. Sadler, *J. Med. Chem.*, 2001, **44**, 3616; (*b*) K. Y. Yan, M. Melchart, A. Habtemariam and P. J. Sadler, *Chem. Commun.*, 2005, 4764; (*c*) O. Novakova, H. M. Chen, O. Vrana, A. Rodger, P. J. Sadler and V. Brabec, *Biochemistry*, 2003, **42**, 11544.
10 M. F. Brana, M. Cacho, A. Gradillas, B. de Pascual-Teresa and A. Ramos, *Curr. Pharma. Des.*, 2001, **7**, 1745.
11 *Cisplatin, Chemistry and Biochemistry of a Leading Anti-Cancer Drug*, ed. B. Lippert, Wiley-VCH, Weinheim, 1999, and references therein.
12 I. Meistermann, V. Moreno, M. J. Prieto, E. Molderheim, E. Sletten, S. Khalid, P. M. Rodger and M. J. Hannon, *Proc. Natl. Acad. Sci. U. S. A.*, 2002, **99**, 5069.
13 (*a*) D.-L. Ma, C.-M. Che, F.-M. Siu, M. Yang and K.-Y. Wong, *Inorg. Chem.*, 2007, **46**, 740; (*b*) H.-L. Chan, H.-Q. Liu, B.-C. Tzeng, Y.-S. You, S.-M. Peng, M. Yang and C.-M. Che, *Inorg. Chem.*, 2002, **41**, 3161; (*c*) J. Liu, X.-H. Zou, Q.-L. Zhang, W.-J. Mei, J.-Z. Liu and L.-N. Ji, *Met-Based Drugs*, 2000, **7**, 343.
14 U. Pindur, M. Haber and K. Sattler, *J. Chem. Educ.*, 1993, **70**, 263.
15 P. M. Bradley, A. M. A. Boza, K. R. Dunbar and C. Turro, *Inorg. Chem.*, 2004, **43**, 2450.
16 (*a*) C. V. Kumar, J. K. Barton and N. J. Turro, *J. Am. Chem. Soc.*, 1985, **107**, 518; (*b*) A. E. Friedman, J. C. Chambron, J. P. Sauvage, N. J. Turro and J. K. Barton, *J. Am. Chem. Soc.*, 1990, **112**, 4960; (*c*) C. Turro, S. H. Bossmann, Y. Jenkins, J. K. Barton and N. J. Turro, *J. Am. Chem. Soc.*, 1995, **117**, 9026.
17 (*a*) C. J. Murphy, M. R. Arkin, Y. Jenkins, N. D. Gathlia, S. H. Bossmann, N. J. Turro and J. K. Barton, *Science*, 1993, **262**, 1025; (*b*) B. Onfelt, P. Lincoln and B. Norden, *J. Am. Chem. Soc.*, 2001, **123**, 3630.
18 (*a*) P. U. Maheswari, V. Rajendiran, R. Parthasarathi, V. Subramanian and M. Palaniandavar, *J. Inorg. Biochem.*, 2006, **100**, 3; (*b*) P. U. Maheswari, V. Rajendiran, H. S. Evans and M. Planiandavar, *Inorg. Chem.*, 2006, **45**, 37; (*c*) B. Selvakumar, V. Rajendiran, P. U. Maheswari, H. S. Evans and M. Palaniandavar, *J. Inorg. Biochem.*, 2006, **100**, 316.
19 E. Amtmann, M. Zoller, H. Wesch and G. Schilling, *Cancer Chemother. Pharmacol.*, 2001, **47**, 461.
20 (*a*) M. Murali and M. Palaniandavar, *Dalton Trans.*, 2006, 730; (*b*) M. Murali and M. Palaniandavar, *Polyhedron*, 2007, **26**, 3980.
21 (*a*) W. I. Sundquist and S. J. Lippard, *Coord. Chem. Rev.*, 1990, **100**, 293; (*b*) F. Wang, H. Chen, J. A. Parkinson, P. del. S. Murdoch and P. J. Sadler, *Inorg. Chem.*, 2002, **41**, 4509; (*c*) A. Egger, V. B. Arion, E. Reisner, B. Cebrian-Losantos, S. Shova, G. Trettenhahn and B. K. Keppler, *Inorg. Chem.*, 2005, **44**, 122.
22 (*a*) J. G. Collins, A. D. Sleeman, J. R. Aldrich, I. Greguric and T. W. Hambley, *Inorg. Chem.*, 1998, **37**, 3133; (*b*) C. M. Dupureur and J. K. Barton, *Inorg. Chem.*, 1997, **36**, 33.
23 M. J. Root and E. Deutsch, *Inorg. Chem.*, 1985, **24**, 1464.
24 V. D. Parker, *Electroanalytical Chemistry*, ed. A. J. Bard, Marcel Dekker, New York, 1989, vol. 14, p. 18.
25 C. Merill, D. Goldman, S. A. Sedman and M. H. Ebert, *Science*, 1980, **211**, 1437.
26 H. A. Goodwin and F. Lions, *J. Am. Chem. Soc.*, 1960, **82**, 5013.
27 M. Vaidyanathan, R. Balamurugan, U. Sivagnanam and M. Palaniandavar, *J. Chem. Soc., Dalton Trans.*, 2001, 3498.
28 *SMART Software,*Seimens Analytical X-ray Instruments Inc., Madison, WI, USA, 1995.
29 L. H. Straver and A. J. Schierbeek, *MolEN, Structure Determination System, Program Description*, Nonius B. V., Delft, 1994, vol. 1, p. 180.
30 (*a*) G. M. Sheldrick, *SHELXS-97: Program for the Solution of Crystal Structure*, University of Göttingen, Göttingen, Germany, 1997; (*b*) G. M. Sheldrick, *SHELXS-97: Program for the Refinement of Crystal Structure*, University of Göttingen, Göttingen, Germany, 1997.
31 *Persistence of Vision Raytracer (Version 3.6)*, Vision Raytracer Pty. Ltd., Scotland, 2004. Retrieved from http://www.povray.org/download/.
32 *SAINT* 5.1, Siemens Industrial Automation Inc., Madison, WI, 1995, G. M. Sheldrick.
33 *SADABS, Empirical Absorption Correction Program*, University of Göttingen, Göttingen, Germany, 1997.
34 G. M. Sheldrick, *SHELXTL Reference Manual: Version 5.1*, Bruker AXS, Madison, WI, 1997.
35 J. Bernadou, G. Prativiel, F. Bennis, M. Girardet and B. Meunier, *Biochemistry*, 1989, **28**, 7268.
36 S. Das, S. Nama, S. Anthony and K. Somasundaram, *Cancer Gene Ther.*, 2005, **2**, 417.
37 N. Wajapeyee and K. Somasundaram, *J. Biol. Chem.*, 2003, **278**, 52093.
38 M. Blagosklonny and W. S. El-Diery, *Int. J. Cancer*, 1996, **67**, 386.
39 J.-Z. Wu, B.-H. Ye, L. Wang, L.-N. Ji, J.-Y. Zhou, R.-H. Li and Z.-Y. Zhou, *J. Chem. Soc., Dalton Trans.*, 1997, 1395.
40 S. Roche, H. Adams, S. E. Spey and J. A. Thomas, *Inorg. Chem.*, 2000, **39**, 2385.
41 D. P. Rillema, D. G. Taghdiri, D. S. Jones, C. D. Keller, L. A. Worl, T. J. Meyer and H. A. Levy, *Inorg. Chem.*, 1987, **26**, 578.
42 R. Hage, J. G. Haasnoot, H. A. Nienwenhuis, J. Reedijk, D. J. A. deRidder and J. G. Vos, *J. Am. Chem. Soc.*, 1990, **112**, 9245.
43 M. J. Cook, A. P. Lewis and G. S. G. McAuliffe, *Org. Magn. Reson.*, 1984, **22**, 388.
44 K. Jitsukawa, Y. Oka, S. Yamaguchi and H. Masuda, *Inorg. Chem.*, 2004, **43**, 8119.
45 (*a*) P. J. Steel, F. Lahousse, D. Lerner and C. Marzin, *Inorg. Chem.*, 1983, **22**, 1488; (*b*) A. J. Downard, G. E. Honey and P. J. Steel, *Inorg. Chem.*, 1991, **30**, 3733; (*c*) G. Orellena, C. A. Ibarra and J. Santoro, *Inorg. Chem.*, 1988, **27**, 1025.
46 (*a*) A. Greguric, I. D. Greguric, T. W. Hambley, J. R. Aldrich-Wright and J. G. Collins, *J. Chem. Soc., Dalton Trans.*, 2002, 849; (*b*) Q.-X. Zhen, B.-H. Ye, J.-G. Liu, Q.-L. Zhang, L.-N. Ji and L. Wang, *Inorg. Chim. Acta*, 2000, **303**, 141.


 

47 (*a*) K. A. O'Donoghue, J. M. Kelly and P. E. Kruger, *Dalton Trans.*, 2004, 13; (*b*) J. R. Aldrich-Wright, R. F. Fenton, I. D. Greguric, T. W. Hambley and P. A. Williams, *J. Chem. Soc., Dalton Trans.*, 2002, 4666.
48 C. Brevard and P. Granger, *Inorg. Chem.*, 1983, **22**, 532.
49 X. Xiaoming, M. A. Haga, T. M. Inoue, Y. Ru, A. W. Addison and K. Kano, *J. Chem. Soc., Dalton Trans.*, 1993, 2477.
50 E. M. Proudfoot, P. Karuso, R. S. Vagg, K. A. Vickery and P. A. Williams, *Chem. Commun.*, 1997, 1623.
51 S. P. Foxon, C. Metcalfe, H. Adams, M. Webb and J. A. Thomas, *Inorg. Chem.*, 2007, **46**, 409.
52 R. J. Staniewicz, R. F. Sympson and D. G. Hendricker, *Inorg. Chem.*, 1977, **16**, 2166.
53 M. N. Ackermann and L. V. Interrante, *Inorg. Chem.*, 1984, **23**, 3904.
54 M. A. Haga, *Inorg. Chim. Acta*, 1983, **75**, 29.
55 H. B. Gray and N. A. Beach, *J. Am. Chem. Soc.*, 1963, **85**, 2922.
56 (*a*) S. Bhattacharya, *Polyhedron*, 1993, **12**, 235; (*b*) D. E. Morris, K. W. Hanckand and M. K. Dearmond, *Inorg. Chem.*, 1985, **24**, 977.
57 D. P. Rillema, G. Allen, T. J. Meyer and D. C. Conrad, *Inorg. Chem.*, 1983, **22**, 1617.
58 (*a*) S. J. Franklin, C. R. Treadway and J. K. Barton, *Inorg. Chem.*, 1998, **37**, 5198; (*b*) A. Chouai, S. E. Wicke, C. Turro, J. Bacsa, K. R. Dunbar, D. Wang and R. P. Thummel, *Inorg. Chem.*, 2005, **44**, 5996.
59 M. T. Carter, M. Rodriguez and A. J. Bard, *J. Am. Chem. Soc.*, 1989, **111**, 8901.
60 R. B. Nair, E. S. Teng, S. L. Kirkland and C. J. Murphy, *Inorg. Chem.*, 1998, **37**, 139.
61 J. G. Liu, B. H. Ye, H. Li, L. N. Ji, R. H. Li and J. Y. Zhou, *J. Inorg. Biochem.*, 1999, **73**, 117.
62 F. M. O'Reilly and J. M. Kelly, *J. Phys. Chem. B*, 2000, **104**, 7206.
63 M. Lee, A. L. Rhodes, M. D. Wyatt, S. Forrow and J. A. Hartley, *Biochemistry*, 1993, **32**, 4237.
64 P. U. Maheswari and M. Palaniandavar, *Inorg. Chim. Acta*, 2004, **357**, 901.
65 M. V. Mikhailov, A. S. Zasedatelev, A. S. Krylov and G. V. Gurskii, *Mol. Biol.*, 1981, **15**, 541.
66 (*a*) B. Weisblum and E. Haenssler, *Chromosoma*, 1974, **46**, 255; (*b*) R. F. Steiner and H. Sternberg, *Arch. Biochem. Biophys.*, 1975, **197**, 580.
67 S. Mahadevan and M. Palaniandavar, *Inorg. Chim. Acta*, 1997, **254**, 291.
68 G. A. Neyhart, N. Grover, S. R. Smith, W. A. Kalsbeck, T. A. Fairley, M. Cory and H. H. Thorp, *J. Am. Chem. Soc.*, 1993, **115**, 4423.
69 C. V. Kumar, J. K. Barton and N. J. Turro, *J. Am. Chem. Soc.*, 1985, **107**, 518.
70 D. H. Johnston, C.-C. Cheng, K. J. Campbell and H. H. Thorp, *Inorg. Chem.*, 1994, **33**, 6388.
71 M. J. Warning, *J. Mol. Biol.*, 1970, **54**, 247.
72 T. W. Welch, A. H. Corbett and H. H. Thorp, *J. Phys. Chem.*, 1995, **99**, 11757.
73 J. Gomez-Segura, M. J. Prieto, M. Font-Bardia, X. Solans and V. Moreno, *Inorg. Chem.*, 2007, **46**, 740.
74 E. C. Long and J. K. Barton, *Acc. Chem. Res.*, 1990, **23**, 271.
75 M. L. Forrest, J. T. Koerber and D. W. Pack, *Bioconjugate Chem.*, 2003, **14**, 934.
76 H. Helmbach, *Int. J. Cancer*, 2001, **93**, 617.
77 D. Grossman, *Cancer Metast. Rev.*, 2001, **20**, 3.
78 G. Li, *Melanoma Res.*, 1998, **8**, 17.
79 R. Osieka, *Cancer Treat. Rev.*, 1984, **11**, 85.
80 S. Lakhani, *Br. J. Cancer*, 1990, **61**, 330.